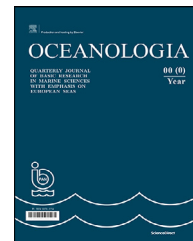


Available online at www.sciencedirect.com

ScienceDirect

journal homepage: www.journals.elsevier.com/oceanologia

ORIGINAL RESEARCH ARTICLE

Distribution and characterization of organic matter within the sea surface microlayer in the Gulf of Gdańsk

Abra Penezić^{a,*}, Violetta Drozdowska^{b,*}, Tihana Novak^a,
Blaženka Gašparović^a

^a Division for Marine and Environmental Research, Rudjer Boskovic Institute, 10000, Zagreb, Croatia

^b Physical Oceanography Department, Institute of Oceanology, Polish Academy of Sciences, Sopot, Poland

Received 23 December 2021; accepted 26 May 2022

Available online 8 June 2022

KEYWORDS

Sea surface microlayer;
Chromophoric dissolved organic matter (CDOM);
Fluorescent organic matter (FDOM);
Surface-active organic substances (SAS);
Marine lipids;
POC

Abstract We present the characterisation and distribution of organic matter (OM) within the sea surface microlayer (SML) and underlying water (ULW) collected in October 2015 at nine stations in the Baltic Sea, Gulf of Gdańsk, encompassing the Vistula River plume. The salinity of >7 throughout the transect indicated Vistula plume was possibly displaced westward by the preceding northerly and easterly winds between 5.7 and 10.7 ms^{-1} during the sampling campaign. Spectral analysis pointed to the highest contribution of aromatic and high molecular weight molecules (lowest spectral slope (S_R) ratios and highest absorption coefficient at 254 nm ($a_{\text{CDOM}}(254)$) at the first two stations near the river mouth, demonstrating a very limited influence of the river plume. Concentrations of surface-active organic substances (SAS) ranged from 0.28 to 0.60 mg L^{-1} in eq. Triton-X-100 in SML, and from 0.22 to 0.47 mg L^{-1} in eq. Triton-X-100 in the ULW, while POC concentrations ranged from 0.27 to 0.84 mg L^{-1} in SML and from 0.20 to 0.37 mg L^{-1} in ULW. Enrichment of SAS and POC detected at the highest wind speeds indicates rapid SML recovery by OM transported from the ULW. Low lipids to POC contribution, on average 5% and 7% in SML and ULW respectively, points to eutrophic conditions. Statistically

* Corresponding authors at: Division for Marine and Environmental Research, Rudjer Boskovic Institute, 10000, Zagreb, Croatia; Physical Oceanography Department, Institute of Oceanology, Polish Academy of Sciences, Sopot, Poland.

E-mail addresses: abra@irb.hr (A. Penezić), drozd@iopan.pl (V. Drozdowska).

Peer review under the responsibility of the Institute of Oceanology of the Polish Academy of Sciences.



<https://doi.org/10.1016/j.oceano.2022.05.003>

0078-3234/© 2022 Institute of Oceanology of the Polish Academy of Sciences. Production and hosting by Elsevier B.V. This is an open access article under the CC BY-NC-ND license (<http://creativecommons.org/licenses/by-nc-nd/4.0/>).

significant negative correlation between S_R and the Lipid:PIG ratio in SML and ULW suggests the production of lower molecular weight OM by phytoplankton living under favourable environmental conditions. Accumulation of lipid reserves triacylglycerols (TG) in the SML indicates more stressful plankton growth conditions compared to ULW.

© 2022 Institute of Oceanology of the Polish Academy of Sciences. Production and hosting by Elsevier B.V. This is an open access article under the CC BY-NC-ND license (<http://creativecommons.org/licenses/by-nc-nd/4.0/>).

1. Introduction

The sea surface microlayer (SML) is an interface between the sea and the atmosphere that affects the processes of mass and energy exchange between the two compartments (Cunliffe et al., 2013; Wurl et al., 2017) and thus affects the global climate. It is defined as the uppermost layer of the sea, up to 1000 μm thick, whose physical and biogeochemical properties differ from those of the underlying water (Hunter, 1997; Zhang et al., 2003). It can be described as a hydrated, gelatinous film in which in-situ produced organic matter (OM) and microorganisms from the deeper layers accumulate along with atmospherically deposited material and pollutants (Engel et al., 2017; Gašparović et al., 1998; Penezić et al., 2021; Robinson et al., 2019; Wurl and Obbard, 2004; Wurl et al., 2017). The formation, thickness and distribution of SML is strongly influenced by meteorological conditions including wind speed (Falkowska, 1999; Liss and Duce, 1997; Stolle et al., 2020). However, it is known that SML recovers quickly after physical disruption (Dragičević and Pravić, 1981; Williams, 1986), mainly through rising bubbles containing organic material adsorbed at the surface (Liss, 1975; Stefan and Szeri, 1999; Woolf, 2005; Wurl et al., 2011). Studies have shown that recovery of SML occurs in all the oceans at wind speeds above average oceanic conditions (Archer and Jacobson, 2005; Sabbaghzadeh et al., 2017; Wurl et al., 2009). Such self-sustainability even at higher sea states, caused by increased bubble fluxes acting as a continuous supply of surface-active material to the SML (Sabbaghzadeh et al., 2017), has strong implications for global air-sea CO_2 exchange. Indeed, the presence of surfactants, which are ubiquitous in the oceans, significantly affects the transport rate of gas across the water surface (Broecker et al., 1978; Frew et al., 1990; Mustaffa et al., 2020; Ribas-Ribas et al., 2017; Tsai et al., 2003; Wurl et al., 2011). Recent studies are beginning to quantify the link between surface-active organic substances (SAS) concentration in SML and gas transfer velocity k_w (Pereira et al., 2016; Rickard et al., 2022).

The marine OM originates mainly from phytoplankton activity, with additional contributions from terrestrial sources through riverine inputs (Gašparović et al., 2011). In coastal waters, especially those under the influence of rivers, increased biological activity leads to increased OM production, with about 70% of dissolved OM being of terrestrial origin (Coble, 2007). A significant portion of marine OM is presented by SAS, consisting of recalcitrant material, such as humic substances, or freshly produced biogenic material, namely carbohydrates, proteins, and lipids (Ćosović et al., 1985; Gašparović et al., 2011). Lipid content in phytoplankton ranges from ≤ 1 to 46% of dry weight

(Romankevich, 1984). Phytoplankton exudates, through direct release or zooplankton grazing, metabolic processes, and cell lysis, are the main source of marine lipids, which vary in composition depending on the phytoplankton community and environmental conditions (Novak et al., 2019).

Lipids are important organic biomarkers used to determine OM sources due to their specific functions in different cell types (Parrish, 1988; Parrish et al., 2000). They are less susceptible to degradation than carbohydrates or proteins. Harvey et al. (1995) found that under oxic conditions carbohydrates are recycled within 15 days, proteins within 41 days, and lipids within 77 days. Saturated lipids have been shown to be highly resistant to degradation. Gašparović et al. (2016, 2018) found an increase in saturated lipids of up to 30-fold from the surface to abyssal depths (4800 m) of the North Atlantic, while at the same time particulate organic carbon decreased by 90%. Membrane lipids, such as phospholipids and glycolipids, are indicators of living organisms, free fatty acids can indicate degradation processes, while the ratio between specific lipid classes can serve as an indicator of organisms' adaptation to changes in environmental conditions (Derieux et al., 1998; Gašparović et al., 2014, 2016; Gerin and Goutx, 1994; Goutx et al., 2003; Novak et al., 2019). Lipids are also an important factor in carbon sequestration in the ocean – their buoyancy contributes to their surface activity, facilitating both their accumulation at the sea surface and their adsorption to sinking particles, which transports them to deeper layers (Gašparović et al., 2016; Novak et al., 2019). Some organic molecules, especially fulvic and humic acids, can absorb light due to their optically active parts, and are referred to as chromophoric dissolved organic matter (CDOM), a class of molecules additionally including fluorescent dissolved organic matter (FDOM), which can emit part of the absorbed light as fluorescence (Drozdowska et al., 2015; Marcinek et al., 2020). As an important optical constituent of seawater, CDOM absorbs primarily in the ultraviolet to the blue spectral region and can absorb up to 90% of solar radiation in the 400–500 nm spectral range in coastal waters, which can affect primary production (Arrigo and Brown, 1996; Belanger et al., 2008; Zhao et al., 2018). Optical characterization methods of OM provide a rapid and reliable way to detect and identify dissolved organic matter (DOM) and additionally give insight into DOM transformation processes (Drozdowska et al., 2017; Stedmon et al., 2003) such as DOM removal through photodegradation or microbial activities (Lei et al., 2020). This is particularly important for coastal areas with intense riverine inputs and high primary production, where optical characterization can help distinguish between DOM of marine and terrestrial origin (Coble, 1996; Drozdowska, 2007; Marcinek et al.,

2020). Biotic and abiotic OM processing at the air–sea interface impacts the ocean carbon cycle (Johannessen et al., 2001) and leads to the formation of volatile organic compounds (VOC), which are potential precursors for secondary organic aerosols (SOA) that strongly influence cloud formation and contribute to Earth's solar radiation balance (Bruggemann et al., 2018; Mayer et al., 2020). The mentioned processes, such as air–water gas exchange, carbon sequestration, VOC formation and others, are of global importance, and are all affected by OM distribution and processing, with different OM classes playing their own important roles in the exchange of energy and matter between the sea and the atmosphere. Therefore, characterization of the marine OM, especially considering the air–sea interface, is essential to deepen our understanding of the feedback between these two largest environmental niches.

In this study, we primarily focused on investigating the links between different organic matter classes within the SML and the underlying water (ULW) at 1 m depth, in the Gulf of Gdańsk, a coastal area in the southern part of the Baltic Sea, influenced by the Vistula River. This study is an extension of the work of Drozdowska et al. (2017), which compared the spectroscopic and fluorescence properties of SML and ULW samples during three different field campaigns (in April 2015, October 2015, and September 2016) collected at the same transect. During the October 2015 campaign, in addition to CDOM and FDOM analysis, additional characterization of OM in the SML and ULW was performed, namely SAS, particulate organic carbon (POC), and particulate lipids and their classes, with the aim of further exploring the specific links between different OM groups and properties, in addition to considering the influence of wind, an important driver of the physical and biogeochemical properties of SML. Thus, the objectives of this study were i) to investigate the properties and spatial distribution of different types of OM in the SML and ULW in a transect in the Gulf of Gdańsk encompassing the Vistula River plume, ii) to identify sources of OM, iii) to identify processes responsible for the distribution of OM and to evaluate the influence of winds on the establishment of SML, and iv) to investigate the relationships between the OM optical properties and OM surface activity.

2. Material and methods

2.1. Study area

The study area included a transect in the southern Baltic Sea, more specifically in the Gulf of Gdańsk, starting at the Vistula River mouth and extending about 47 km toward the open sea (Figure 1, Table S1). The brackish Baltic Sea is characterised by a high water residence time due to poor exchange with the North Sea through the Danish Straits (Szymczak-Żyła et al., 2019). This and its large catchment area make it vulnerable to eutrophication, anoxia, and the impacts of pollutants (Pędziniński and Witak, 2019; Szymczak-Żyła et al., 2019). Between the early and late 20th century intensive inputs of nitrogen and phosphorus increased four-fold and eightfold, respectively (Glasby and Szefer, 1998; Larsson et al., 1985), promoting eutrophication, reducing water transparency, and causing a shift from macrophyte- to phytoplankton-dominated systems in some areas of the

Baltic Sea (Andrén, 1999). Vistula River, the longest river in the Baltic Sea catchment, with a length of 1047 km and an average flow of 1080 m³ s⁻¹ (Buszewski et al., 2005), brings the largest amounts of total nitrogen and phosphorus (about 65 and 60%, respectively) (HELCOM, 2018) and, despite recent reductions in nutrient inputs (HELCOM, 2018; Pastuszek et al., 2012), contributes to eutrophication, especially in the Gulf of Gdańsk area. The Gulf of Gdańsk is a highly eutrophic area with large-scale growth of filamentous brown algae, extensive summer blooms of cyanobacteria, and high Chl *a* concentrations (Kruk-Dowgiallo, 1996; Mazur-Marzec et al., 2006). Due to the considerable input of terrestrial OM, which affects its optical and biological properties (Kowalczyk et al., 2006), the Gulf of Gdańsk has also been recognized as a sink for particulate matter of both autochthonous and allochthonous origin (Drozdowska et al., 2002; Drozdowska and Fateyeva, 2013; Maksymowska et al., 2000; Piskozub et al., 1998). The dynamic conditions of this coastal area make it particularly interesting as a study site for the characterisation of different OM classes and their interactions.

2.1.1. Sampling and sample treatment

Sampling was conducted at nine stations (Figure 1) between October 15th and 16th, 2015. The exact locations of the stations, indicated by W1–W9, are given in Table S1. The ULW samples were collected from a depth of 1 m, using a 10 L Niskin water sampler, while the SML samples were collected using a 50 × 50 cm stainless steel Garret net, mesh size 18 (a wire thickness 0.36 mm and the mesh eye size 1 mm), which approximates the thickness of the collected SML to 500 μm. The SML sampling procedure is described in detail in Drozdowska et al. (2017) and in the Supplementary Information (Figure S1). Briefly, samples were collected from onboard the *r/v Oceania*, by vertically immersing the screen and waiting for the microlayer to stabilize before carefully lifting the screen horizontally through the water surface at a speed of approximately 5–6 cm s⁻¹. In windy conditions, it is necessary to hold the ship bow to wind, so that the screw – astern and about 1 m below the water surface – is idling, i.e. spinning slowly, but this does not disturb the stability of the surface water amidships. Exceptionally, during water sampling on this cruise, in high wind conditions, the ship was oriented with its head to the wind to minimize disturbance of the wind field and potential contamination from the ship, while samples were collected from the bow (Sabbaghzadeh et al., 2017; Salter et al., 2011). The shape of the hull of *r/v Oceania*, tapering downwards, allows the surface water to be reached by the Garret Screen from a distance of approximately 1–3 m from the ship's side, further minimizing potential contamination. The samples were poured into polyethylene bottles through a special slit in the screen frame. Aliquots of the collected samples were used for the determination of SAS, which were determined on board immediately after sampling and without filtration. Aliquots collected for absorbance and fluorescence measurements were placed unfiltered in dark containers and stored at 4°C until measurement within 48 h of sampling. Aliquots for particulate lipid measurements were first filtered through a metal mesh with a pore size of 200 μm to avoid sampling organisms larger than phytoplankton and large organic particles. Samples were then filtered through

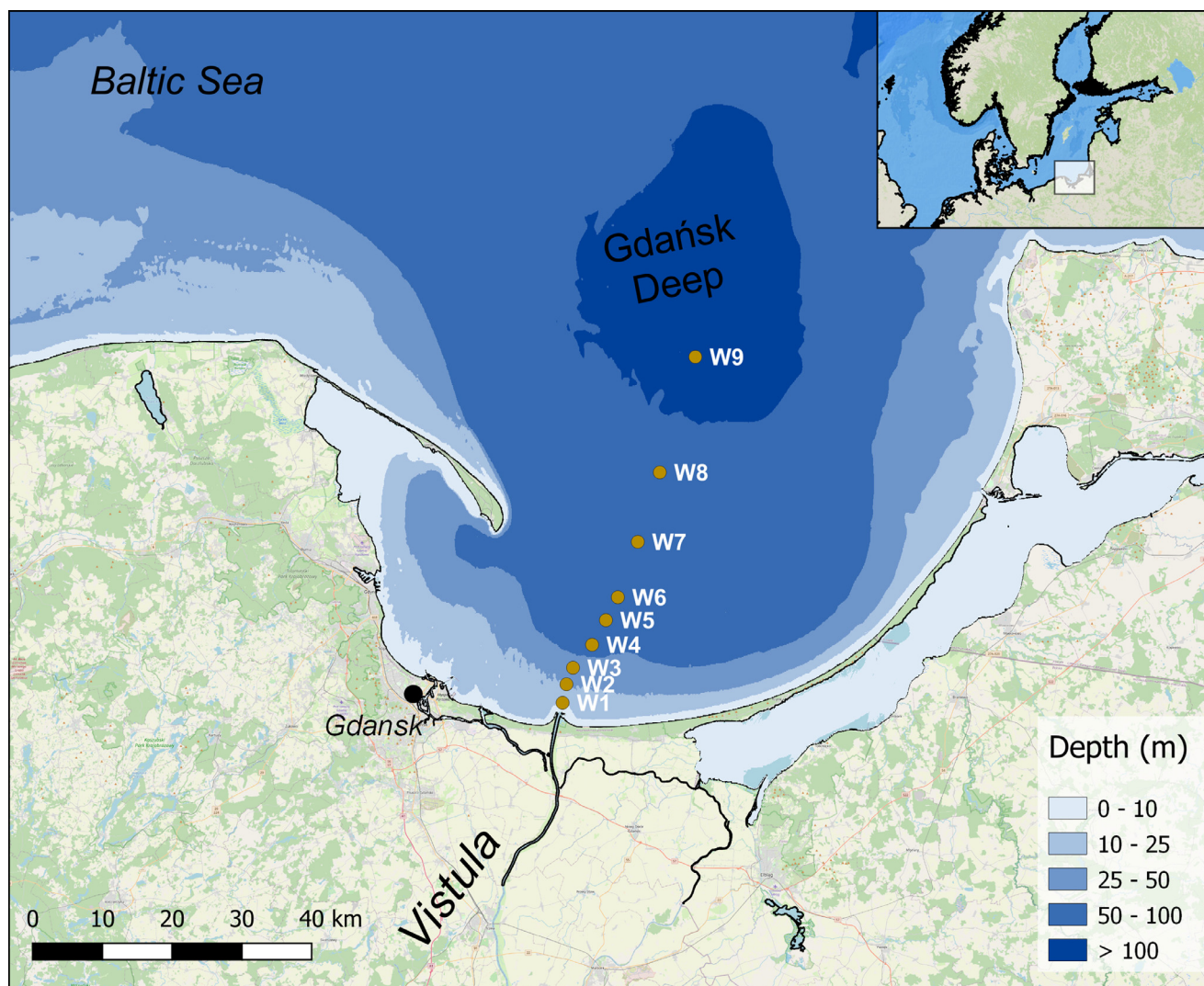


Figure 1 Sampling stations (W1–W9) in the Gulf of Gdańsk, the southern Baltic Sea. Map made with QGIS (QGIS Development Team 2018; <http://qgis.osgeo.org>, accessed on November 12th, 2021).

glass fibre filters with a pore size of $0.7 \mu\text{m}$ (GF/F Whatman, Buckinghamshire, UK). The filters were then placed in cryotubes, frozen in liquid nitrogen and stored at -20°C until analysis. Prior to use, the filters were pre-burned at 450°C for 4 hours to remove possible organic contaminants. The same filter types and storage procedure were used to collect the POC samples. All glassware used for filtration was washed with chromic sulfuric acid and rinsed with ultrapure water (Merck Millipore, Burlington, Massachusetts, USA) to avoid organic contaminants. Salinity and sea surface temperature were measured during sampling at a depth of 0.6–0.9 m, using a CTD probe (SeaBird SBE 49, Bellevue, Washington, USA).

2.1.2. Statistical analysis

Pearson's correlation coefficient matrix was used to test correlations between different parameters, while two-sample t-test was used to test for significant differences between datasets means. Statistical analysis was done in Origin 7 (Origin Lab, USA).

2.2. Organic matter analysis

2.2.1. Particulate organic carbon analysis

POC was determined using an SSM-5000A solid sample module, connected to a TOC-VCPH (Shimadzu, Japan) carbon analyser calibrated with glucose. Samples were acidified with 2 mol L^{-1} HCl, to remove the inorganic carbonate fraction, folded, and placed in alumina ceramic sample boats, followed by drying at 50°C for 12 hours (Giani et al., 2005; Ryba and Burgess, 2002). The samples were then burned at 900°C in a stream of oxygen. The produced CO_2 is detected using a non-dispersive infrared (NDIR) detector. POC concentrations were corrected using measurements of blank filters, which were subjected to the same procedure as the samples. The value obtained by the average filter blank, which includes the instrument blank, is $5 \mu\text{g C L}^{-1}$. The calibration was made with glucose standards in the range between 0 and $200 \mu\text{g}$ organic carbon, giving the reproducibility of the method of 3% and a limit of detection of $5 \mu\text{g C L}^{-1}$.

2.2.2. Chromophoric and fluorescent organic matter analysis

The results of chromophoric and fluorescent analysis of organic matter have already been published in the study by Drozdowska et al. (2017), where more details on the analytical procedures can be found, but are also briefly presented here. Samples collected for CDOM and FDOM analysis were not filtered, to characterise the total OM and to maintain consistency with SAS determination, as it is assumed that filtration removes a significant amount of surfactants (Schneider-Zapp et al., 2013). In previous studies, we observed that the differences between filtered and non-filtered samples were in the short UV and far VIS ranges, but did not cause significant changes in the absorption indices, as these were based on the relative differences between the values of $a_{\text{CDOM}}(\lambda)$ determined between the two affected ranges (Drozdowska et al., 2017). Moreover, filtration affects the fluorescence spectral bands only for the protein-type T component, with the differences being the same for SML and ULW (Drozdowska et al., 2018, 2017). Being aware of the limitations of the methods used, we decided to conduct the measurements on the unfiltered samples but to keep the CDOM and FDOM nomenclature (Drozdowska and Józefowicz, 2015).

Absorbance measurements were carried using a Perkin Elmer Lambda 650 spectrophotometer (Perkin Elmer, Waltham, Massachusetts, USA). The uncertainty of the instrument for the absorbance signal is less than 0.001. For a 10 cm path length quartz cuvette, the systematic error of the measurement on the spectrophotometer is constant and is 0.023 cm^{-1} . The recorded spectral range was between 240 and 700 nm using ultrapure water as the reference signal. The recorded absorbance $A(\lambda)$ spectra were processed to obtain CDOM absorption coefficients curves $a_{\text{CDOM}}(\lambda)$, m^{-1} . Next, a non-linear least-squares fitting method was applied (Stedmon et al., 2000) to calculate the spectral slope coefficient ($S_{\Delta\lambda}$) in two spectral ranges: 275–295 and 350–400 nm, $S_{275-295}$ and $S_{350-400}$, respectively. The ratio of the two spectral slope coefficients, $S_{275-295}$ and $S_{350-400}$, is known as the slope ratio (S_R) and serves as an indicator of the molecular weight and source of OM; higher molecular weight molecules, which are also more likely to be of allochthonous origin, have a low S_R (Helms et al., 2008). The standard deviations (SD) of $S_{275-295}$ and $S_{350-400}$ did not exceed 2% of their values, while the maximum uncertainty of the measurement and SD of S_R did not exceed 6% and 3%, respectively.

Fluorescence excitation emission matrix (EEM) spectra were obtained using a Cary Eclipse scanning spectrofluorometer (Agilent Technologies, Santa Clara, California, USA), with samples measured in a 1 cm path length quartz cuvette. A series of emission scans (280–600 nm at 2 nm resolution) were measured over an excitation wavelength range between 250 and 500 nm in 10 nm increments. To standardize fluorescence intensity measurements to Raman units, RU (Murphy et al., 2010), i.e., to ensure comparability of results, a scan of ultrapure water is performed on each measurement day. The EEM spectrum of the ultrapure water allows control of instrument parameters and to count the energy of the Raman scattering band between 375–425 nm, for the spectrum excited at 350 nm. The calculated value is

used to correct the EEM spectra of the SML and ULW water samples.

2.2.3. Lipid analysis

Lipid material collected on GF/F filters was extracted by using a modified procedure described by Bligh and Dyer (1959), with n-hexadecanone added as an external standard for calculating the sample recovery. The detailed procedure is explained in Gašparović et al. (2014, 2015, 2017) and is briefly presented here. Lipid extracts were evaporated to dryness under a stream of nitrogen and redissolved in 14 to 20 μL of dichloromethane. Aliquots of 2 μL of the redissolved sample were spotted onto silica-coated quartz thin-layer chromatography rods, where the samples were developed in a series of seven developing baths with a mixture of increasingly polar organic solvents. After development, lipids were analysed using a thin layer chromatography – flame ionization detector (TLC-FID) Iatroscan MK-VI (Iatron, Japan) at a hydrogen flow rate of 160 ml min^{-1} and an air flow rate of 2000 ml min^{-1} , and quantified using external calibration with lipid class standards. Each sample was analysed between two and four times. Limits of detection (LODs) were determined as the analyte concentrations corresponding to a signal-to-noise (S/N) ratio of 3. The lipid classes analysed and their LODs are as follows: hydrocarbons (HC), LOD = 0.10 μg ; triacylglycerols (TG), LOD = 0.20 μg ; wax and sterol esters (WE), LOD = 0.10 μg ; fatty acid methyl esters (ME), LOD = 0.22 μg ; ketones (KET), LOD = 0.25 μg ; free fatty acids (FFA), LOD = 0.15 μg ; fatty alcohols (ALC), LOD = 0.20 μg ; 1,3-diacylglycerols (1,3 DG), LOD = 0.33 μg ; sterols (ST), LOD = 0.15 μg ; 1,2-diacylglycerols (1,2 DG), LOD = 0.15 μg ; pigments (PIG), LOD = 0.25 μg ; monoacylglycerols (MG), LOD = 0.15 μg ; monogalactosyldiacylglycerols (MGDG) LOD = 0.23 μg , digalactosyldiacylglycerols (DGDG), LOD = 0.21 μg ; sulfoquinovosyldiacylglycerols (SQDG), LOD = 0.06 μg ; mono- and di-phosphatidylglycerols (PG), LOD = 0.27 μg , phosphatidylethanolamines (PE), LOD = 0.11 μg ; and phosphatidylcholines (PC), LOD = 0.14 μg . The percent recoveries of the samples were calculated from the ratio of the recovered n-hexadecanone mass and the theoretical n-hexadecanone mass originally added to the sample. The recovery averaged $117 \pm 16\%$. The final concentration of particulate lipid (C) was then calculated based on the mass of lipid (m) obtained with the calibration equations, the volume of the sampled seawater (V_{sample}), the percentage of the spotted sample (% spotted), and the lipid recovery (% recovery) using the following equation:

$$C = \frac{\frac{(m \times 100)/(\% \text{ spotted})}{V_{\text{sample}}} \times 100}{\% \text{ recovery}} \quad (1)$$

2.2.4. Surface-active substances analysis

Surface-active substances were determined electrochemically by alternating current (AC) voltammetry (Ćosović, 2005; Ćosović and Vojvodić, 1998) using a portable potentiostat (Palmsens, Houten, The Netherlands). The three-electrode system consisted of a hanging mercury drop working electrode, an Ag/AgCl (3M KCl) reference electrode, and a platinum wire counter electrode. Only the capacitive component of the current is measured by AC voltammetry

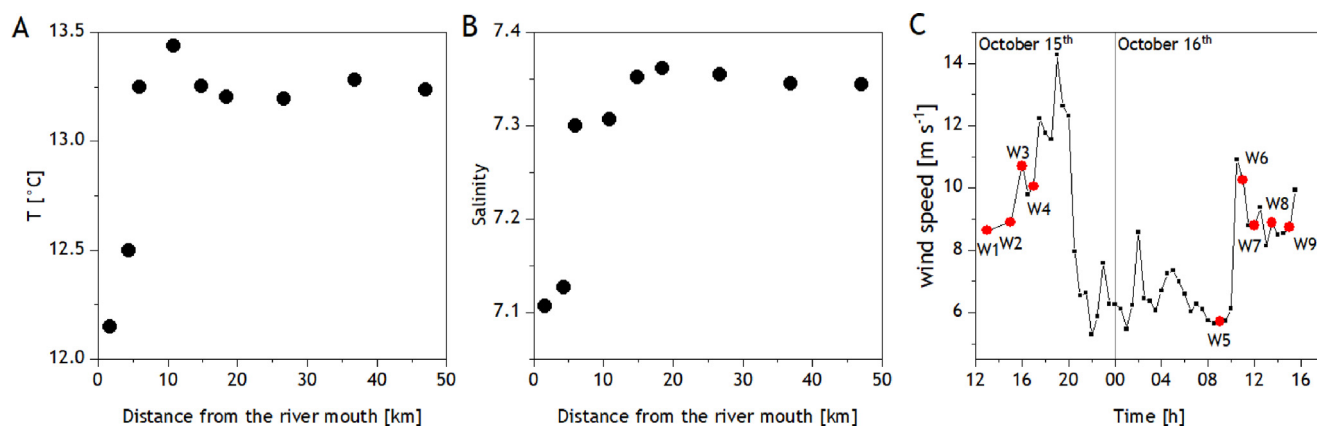


Figure 2 Sea surface temperature (A) and salinity (B), along with average wind speed (C) recorded throughout the field campaign and the transect.

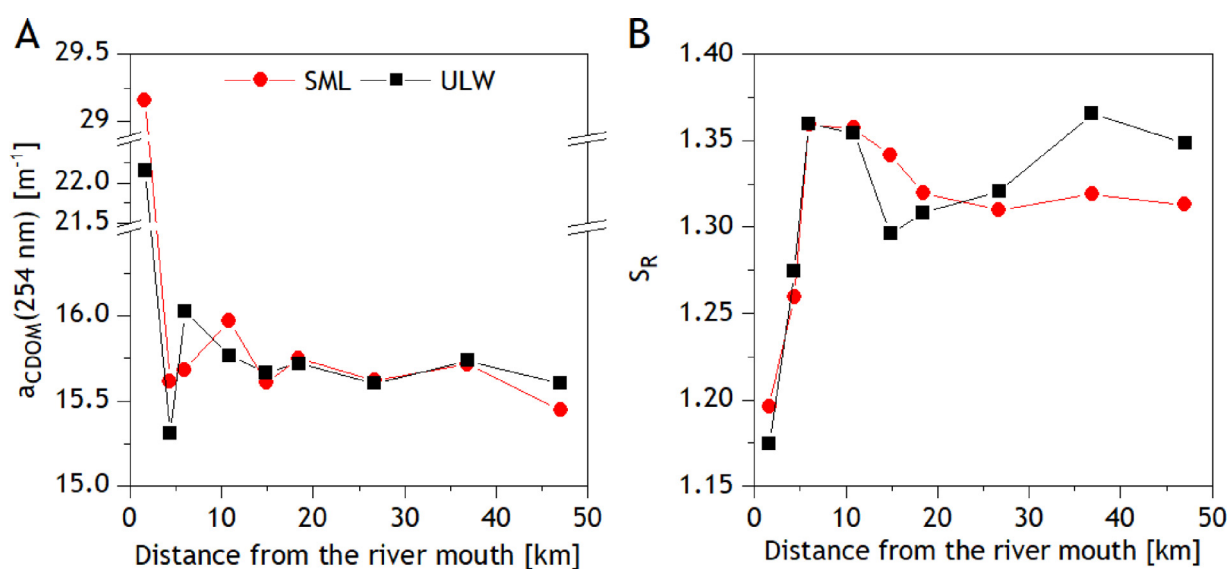


Figure 3 The CDOM absorption coefficient at 254 nm, $a_{\text{CDOM}}(254)$ (A) and spectral slope ratio (S_R) (B) determined for sea surface microlayer (SML) (circles) and underlying water (ULW) (squares) samples.

and the concentration of SAS is estimated from calibration curves obtained with a nonionic surfactant Triton-X-100 (T-X-100), which serves as a good model compound (Frka et al., 2009). Calibration was performed in 0.5 M NaCl, and the determined LOD of the method was 0.07 mg L⁻¹ eq. Triton X-100. The ionic strength of the samples was adjusted to 0.5 M by adding saturated NaCl before the measurements.

3. Results

3.1. Oceanographic parameters

Data on sea surface temperature and salinity, along with wind speed are shown in Figure 2. The lowest temperatures, 12.1 and 12.5°C, were measured at stations W1 and W2, which are closest to the river mouth. Thereafter, a slight increase was observed, and the temperature remained between 13.2 and 13.4°C throughout the transect. Salinity

was lowest near the river mouth at stations W1 and W2, at about 7.1, which is, however, higher than expected for the Vistula Estuary and indicates a strong mixing of the fresh and seawater (Drozdowska et al., 2017; Schiewer and Schernewski, 2002). This was to be expected as meteorological conditions in October 2015 just prior to the field campaign included a strong northerly wind blowing from the open Baltic Sea to the coast of Poland, which changed to predominantly easterly winds throughout the field campaign. The presence of easterly/south-easterly winds and westerly surface currents (Figure S2) may have shifted the Vistula plume to the west of the studied transect. Therefore, the influence of the river was difficult to discern. Only the slightly lower salinity at stations near the river mouth, e.g., W1 and W2, indicated the influence of the Vistula plume. At the times of sampling, which was performed mainly in the afternoon hours (Table S1), wind speed varied between 5.7 m s⁻¹ and 10.7 m s⁻¹ with values mostly above 8.5 m s⁻¹. The lowest wind speed was observed after a calm night between

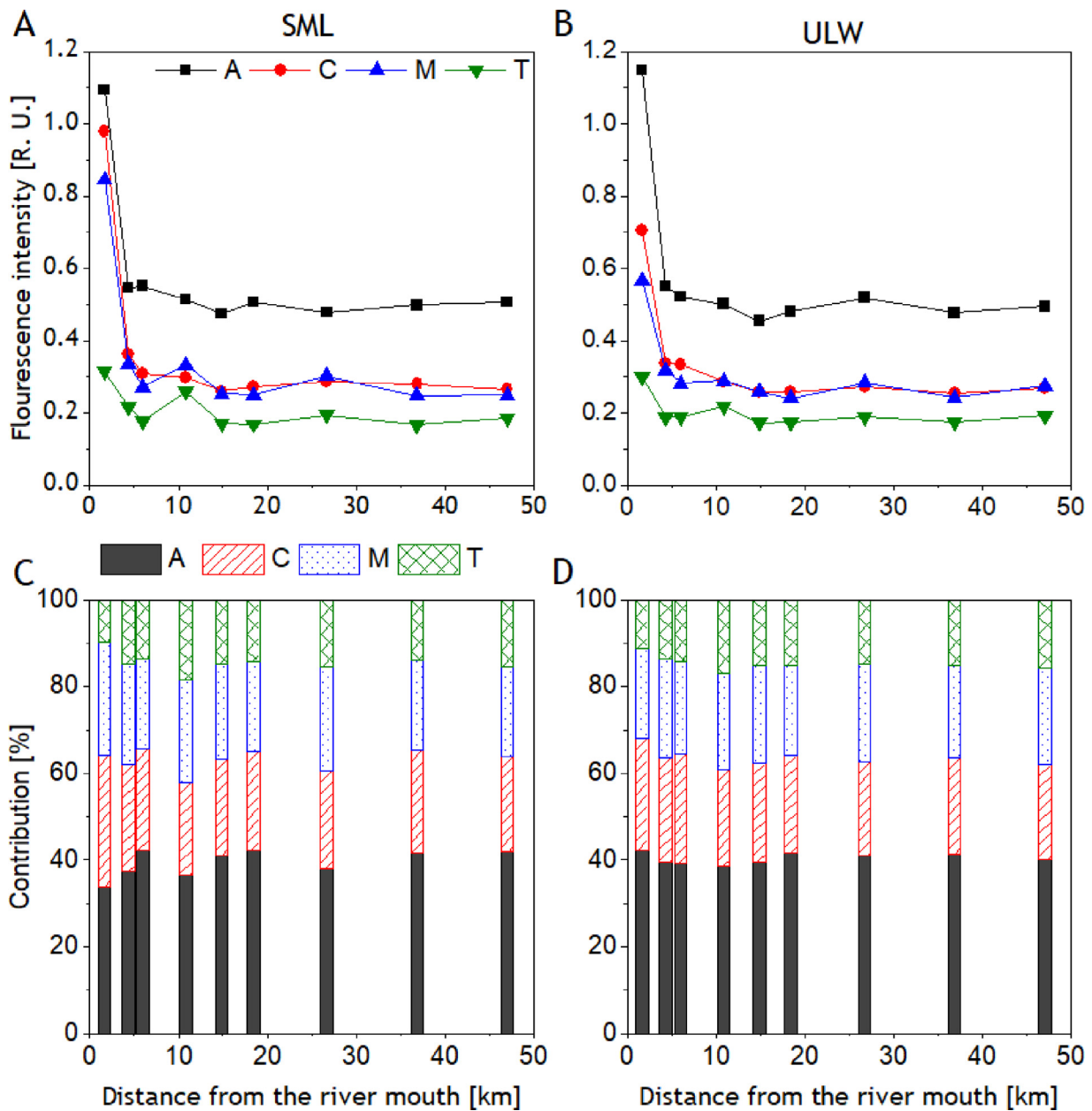


Figure 4 Fluorescence intensities of main FDOM components (A and B) and percentage composition of terrestrial UV humic-like substances (A), terrestrial visible humic-like substances (C), marine humic-like substances (M), and proteinaceous substances (T) (C and D) of the sea surface microlayer (SML) (A and C) and underlying water (ULW) (B and D) throughout the transect.

October 15th and 16th, which resulted in sample W5 being sampled during the calmest conditions of the field campaign (Figure 2).

3.2. Chromophoric organic matter

Based on the UV/VIS spectra of SML and ULW samples, the absorption coefficients at 254 nm ($a_{CDOM}(254)$) were determined (Figure 3), which are specific for aromatic molecules absorbing at this wavelength. The highest $a_{CDOM}(254)$ in SML was determined at station W1, followed by a significant decrease at W2, with the lowest $a_{CDOM}(254)$ determined at station W9, farthest from the Vistula River. A similar distribu-

tion was observed in the ULW, with the highest $a_{CDOM}(254)$ determined at W1, and a significant decrease at W2, which was in fact the lowest observed $a_{CDOM}(254)$ value in the ULW. The slope ratio (S_R) in the SML ranged from 1.20 at station W1 to 1.36 at stations W3 and W4, while in ULW the lowest ratio was also observed at station W1 (1.17) and the highest at W8 (1.37).

Fluorescence intensities and contribution of each component to FDOM composition in the SML and ULW are shown in Figure 4. Fluorescence intensities of the major FDOM components: A, C, M and T, expressed in Raman units (R. U.), are used as proxies of the different FDOM types. Peak A is attributed to terrestrial UV humic-like

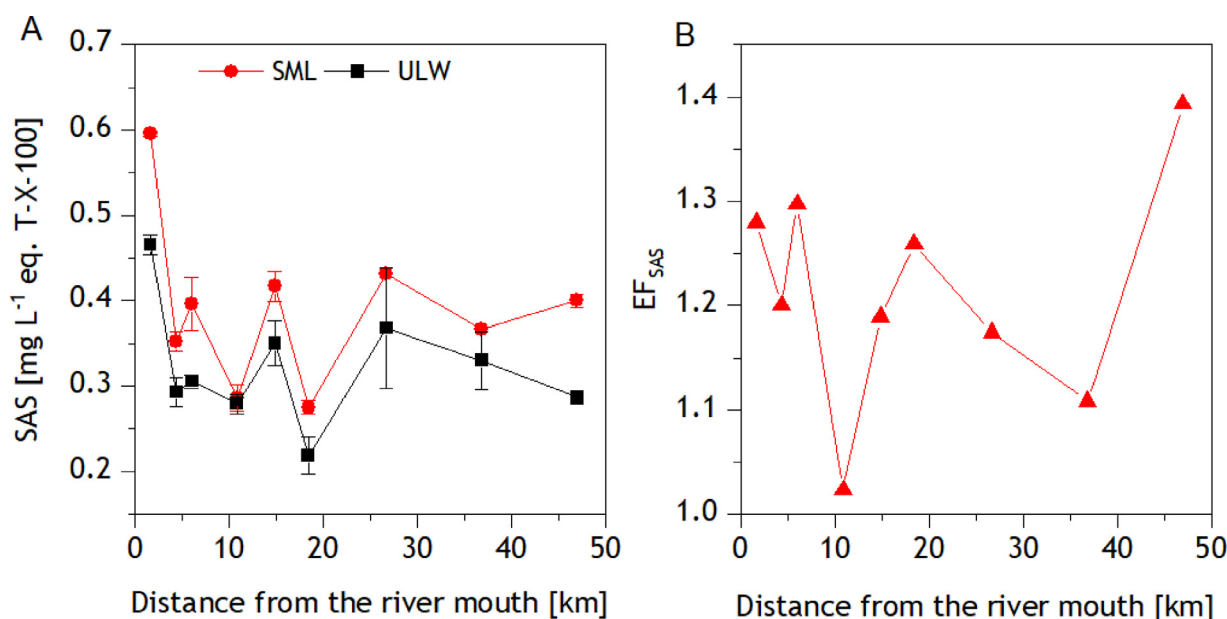


Figure 5 Distribution of surface-active organic substances (SAS) in the sea surface microlayer (SML) (circles) and underlying water (ULW) (squares) (A) and SAS enrichment factors (B) throughout the transect.

substances (ex./em. – excitation and emission – 250/437 nm); peak C represents terrestrial visible-humic like substances (ex./em. 310/429 nm); peak M characterizes marine humic-like substances (ex./em. 300/387 nm) and peak T represents proteinaceous substances (ex./em. 270/349 nm) (Loiselle et al., 2009; Zhang et al., 2013a). The values of the (M+T):(A+C) ratios are given in Table S2. The ratios allow an assessment of the relative contribution of DOM recently produced in situ (M+T) to terrestrial humic substances (A+C), which are characterized by highly complex structures with high molecular weight (Parlanti et al., 2000). Values of the ratio (M+T):(A+C) >1 indicate the predominance of autochthonous DOM, while values of <0.6 indicate allochthonous/anthropogenic DOM (Drozdowska et al., 2015).

The levels of FDOM components were only slightly higher in the SML than in the ULW. The difference between the means in SML and ULW was not statistically significant according to the two-sample t-test. The percent composition of FDOM components varied most within the first 15 km of the transect at stations W1–W4, while in the remainder of the transect the contributions of each component remained fairly constant in both SML and ULW. The contribution of UV humic-like substances (A) averaged 40% in both SML and ULW. In the SML it ranged from 34% at W1 to 42% at W3 and in ULW from 39% at W3 to 42% at W1. Terrestrial visible humic-like substances (C) contributed an average of 24% in the SML and 23% in the ULW to FDOM composition and were highest at W1, near the river mouth, in both SML and ULW. They ranged from 21% at W3 to 30% at W1 in SML, and from 22% at W7 to 26% at W1 in ULW. Marine humic-like substances (M) contributed an average of 22% to the FDOM composition of SML and ULW, ranging from 21% at W9 to 26% at W1 in the SML, and from 21% at W1 to 23% at W2 in the ULW. The contribution of proteinaceous material (T) was distributed differently compared to other components. At station W1, their contribution was lowest in both SML and ULW, 10% and

11%, respectively, while the highest contribution was found at station W4, 18% and 17% in the SML and ULW, respectively. The average contribution of proteinaceous material across the transect was 15% in both SML and ULW.

3.3. Surface-active substances

Concentrations of SAS in the SML and ULW throughout the transect are shown in Figure 5A and listed in Table S2. Concentrations in the SML ranged from 0.28 ± 0.01 mg L⁻¹ to 0.60 ± 0.00 mg L⁻¹ in eq. T-X-100, with an average value of 0.39 ± 0.09 mg L⁻¹ in eq. T-X-100, while in the ULW they ranged from 0.22 ± 0.02 mg L⁻¹ to 0.47 ± 0.01 mg L⁻¹ in eq. T-X-100, with an average value of 0.32 ± 0.07 mg L⁻¹ in eq. T-X-100. The highest concentrations were determined at the river mouth, at station W1, and the lowest at station W6, in both the SML and ULW. A statistically significant positive correlation was found between the concentration of SAS in the SML and in the ULW ($r = 0.937$, $p < 0.001$).

The enrichment factor (EF), defined as the ratio of SAS concentrations determined in the SML and ULW, showed that all SML samples were enriched in SAS (Figure 5B). Enrichment factors ranged from 1.0 to 1.4 (Table 2), with the lowest EF observed at station W4 and the highest at station W9, which is farthest from the river mouth (Figure 5B).

3.4. Particulate organic carbon and particulate lipids

The distribution of POC and particulate lipids in the SML and ULW and the corresponding EFs are shown in Figure 6. The POC value determined at station W4 was extremely low (0.004 mg L⁻¹), suggesting measurement error, and was therefore not considered in further analysis. Table 1 shows the concentrations of total particulate lipids and lipid classes determined in the SML and ULW. POC concentrations

Table 1 Concentrations of particulate total lipids and lipid classes (\pm SD) in the sea surface microlayer (SML) and underlying (ULW) in the analyzed transect.

SML ($\mu\text{g L}^{-1}$)																		
Station	Membrane lipids										Intracellular reserve lipids			Degradation indices				
	Total	HC	ST	PIG	MGDG	DGDG	SQDG	PG	PE	PC	WE	ME	TG	FFA	ALC	1,3 DG	1,2 DG	MG
W1	37.30 \pm 4.07	\pm 1.75	\pm 0.73	\pm 1.14	\pm 1.20	\pm 4.50	\pm 5.09	\pm 3.76	\pm 0.83	\pm 2.13	\pm 0.29	\pm 3.16	\pm 5.76	\pm 0.59	\pm 0.91	\pm 1.38	\pm 0.02	\pm 1.79
	1.79	0.35	0.02	0.04	0.02	0.04	0.23	0.60	0.46	0.12	0.29	0.09	0.02	0.56	0.07	0.01	0.27	0.00
W2	35.80 \pm 2.85	\pm 1.63	\pm 0.73	\pm 3.89	\pm 1.26	\pm 5.12	\pm 4.05	\pm 2.62	\pm 0.81	\pm 1.25	\pm 0.12	\pm 3.39	\pm 5.82	\pm 0.51	\pm 0.45	\pm 1.29	\pm 0.02	\pm 1.82
	0.09	0.14	0.06	0.45	0.07	0.61	0.21	0.04	0.02	0.13	0.05	0.60	0.56	0.05	0.16	0.08	0.00	
W3	28.16 \pm 1.87	\pm 1.35	\pm 0.78	\pm 2.81	\pm 1.61	\pm 2.41	\pm 5.36	\pm 2.07	\pm 0.67	\pm 0.59	\pm 0.23	\pm 3.15	\pm 3.58	\pm 0.58	\pm 0.53	\pm 0.53	\pm 0.05	\pm 1.48
	0.11	0.03	0.10	0.03	0.07	0.38	0.32	0.09	0.06	0.10	0.01	0.24	0.49	0.08	0.05	0.02	0.02	
W4	27.82 \pm 1.75	\pm 1.17	\pm 1.29	\pm 1.67	\pm 1.79	\pm 3.63	\pm 5.35	\pm 2.04	\pm 0.79	\pm 0.54	\pm 0.19	\pm 1.12	\pm 4.69	\pm 0.95	\pm 0.38	\pm 0.44	\pm 0.03	\pm 1.58
	0.02	0.05	0.14	0.06	0.25	0.05	0.71	0.03	0.10	0.21	0.11	0.22	0.42	0.02	0.07	0.03	0.00	
W5	30.65 \pm 4.41	\pm 1.15	\pm 0.70	\pm 1.83	\pm 1.94	\pm 5.70	\pm 4.69	\pm 2.36	\pm 0.85	\pm 0.60	\pm 0.07	\pm 0.83	\pm 3.79	\pm 0.81	\pm 0.43	\pm 0.50	\pm 0.01	\pm 1.94
	0.40	0.03	0.11	0.10	0.20	0.48	1.03	0.10	0.12	0.13	0.02	0.03	0.80	0.08	0.04	0.10	0.00	
W6	33.04 \pm 2.45	\pm 1.13	\pm 0.79	\pm 6.20	\pm 1.56	\pm 5.06	\pm 5.03	\pm 1.86	\pm 0.73	\pm 1.19	\pm 0.05	\pm 1.67	\pm 3.38	\pm 0.62	\pm 0.59	\pm 0.73	\pm 0.01	\pm 1.70
	0.25	0.20	0.13	0.47	0.16	0.39	0.30	0.06	0.01	0.04	0.02	0.13	0.31	0.10	0.07	0.24	0.00	
W7	34.99 \pm 2.21	\pm 1.29	\pm 1.08	\pm 6.23	\pm 1.95	\pm 5.88	\pm 4.19	\pm 2.28	\pm 0.75	\pm 0.78	\pm 0.26	\pm 1.18	\pm 4.83	\pm 0.96	\pm 0.44	\pm 0.67	\pm 0.01	\pm 2.12
	1.18	0.04	0.27	0.14	0.08	0.90	0.34	0.01	0.03	0.16	0.09	0.24	0.39	0.34	0.21	0.07	0.00	
W8	34.20 \pm 2.22	\pm 1.25	\pm 1.08	\pm 4.13	\pm 1.69	\pm 5.78	\pm 5.29	\pm 1.90	\pm 0.96	\pm 0.77	\pm 0.19	\pm 1.10	\pm 5.73	\pm 0.98	\pm 0.42	\pm 0.68	\pm 0.01	\pm 1.69
	0.08	0.06	0.14	0.32	0.06	0.43	0.03	0.17	0.02	0.11	0.13	0.19	0.75	0.01	0.08	0.27	0.00	
W9	31.44 \pm 2.16	\pm 1.35	\pm 0.92	\pm 3.42	\pm 1.80	\pm 5.37	\pm 3.85	\pm 0.95	\pm 0.61	\pm 0.79	\pm 0.36	\pm 2.86	\pm 5.24	\pm 0.61	\pm 0.44	\pm 0.69	\pm <LOD	\pm 1.96
	0.21	0.15	0.38	0.23	0.42	0.84	0.55	0.03	0.09	0.05	0.00	0.05	0.51	0.30	0.01	0.03		

ULW ($\mu\text{g L}^{-1}$)																		
Station	Membrane lipids										Intracellular reserve lipids			Degradation indices				
	Total	HC	ST	PIG	MGDG	DGDG	SQDG	PG	PE	PC	WE	ME	TG	FFA	ALC	1,3 DG	1,2 DG	MG
W1	22.73 \pm 1.54	\pm 1.04	\pm 0.43	\pm 1.10	\pm 0.79	\pm 4.32	\pm 3.33	\pm 3.03	\pm 0.62	\pm 0.62	\pm 0.11	\pm 0.91	\pm 3.31	\pm 0.41	\pm 0.58	\pm 0.54	\pm 0.01	\pm 1.42
	0.05	0.06	0.22	0.02	0.21	0.01	0.26	0.07	0.01	0.06	0.05	0.04	0.61	0.00	0.06	0.28	0.00	
W2	28.66 \pm 1.50	\pm 1.86	\pm 0.47	\pm 1.18	\pm 1.08	\pm 5.07	\pm 3.81	\pm 3.46	\pm 1.00	\pm 0.21	\pm 0.10	\pm 1.81	\pm 5.70	\pm 0.43	\pm 0.29	\pm 0.66	\pm 0.02	\pm 1.61
	0.09	0.11	0.02	0.21	0.14	0.04	0.29	0.48	0.14	0.01	0.03	0.50	0.36	0.08	0.01	0.07	0.00	
W3	25.03 \pm 1.48	\pm 1.06	\pm 1.11	\pm 2.41	\pm 1.64	\pm 2.44	\pm 5.75	\pm 1.72	\pm 0.88	\pm 0.22	\pm 0.18	\pm 1.08	\pm 3.43	\pm 0.91	\pm 0.35	\pm 0.33	\pm 0.05	\pm 1.58
	0.05	0.18	0.01	0.24	0.13	0.55	0.42	0.22	0.03	0.01	0.10	0.19	0.01	0.28	0.05	0.03	0.01	
W4	26.05 \pm 1.47	\pm 1.09	\pm 1.63	\pm 1.81	\pm 1.90	\pm 2.93	\pm 5.36	\pm 2.21	\pm 0.74	\pm 0.24	\pm 0.25	\pm 0.96	\pm 3.66	\pm 0.93	\pm 0.44	\pm 0.42	\pm 0.02	\pm 1.20
	0.15	0.06	0.23	0.08	0.07	0.03	0.04	0.15	0.04	0.02	0.00	0.23	0.24	0.07	0.01	0.01	0.00	
W5	21.50 \pm 1.28	\pm 0.75	\pm 0.85	\pm 1.20	\pm 1.27	\pm 5.11	\pm 4.28	\pm 1.78	\pm 0.63	\pm 0.27	\pm 0.03	\pm 0.62	\pm 2.13	\pm 0.63	\pm 0.23	\pm 0.44	\pm 0.01	\pm 1.86
	0.37	0.19	0.20	0.14	0.10	0.50	0.70	0.09	0.08	0.09	0.04	0.06	0.59	0.09	0.09	0.13	0.00	
W6	28.48 \pm 1.64	\pm 0.90	\pm 0.70	\pm 1.38	\pm 1.84	\pm 5.79	\pm 6.92	\pm 2.28	\pm 0.51	\pm 0.45	\pm 0.16	\pm 0.50	\pm 3.83	\pm 0.73	\pm 0.30	\pm 0.54	\pm 0.01	\pm 2.72
	0.45	0.15	0.22	0.43	0.09	1.39	3.05	0.40	0.02	0.23	0.09	0.08	0.13	0.24	0.18	0.24	0.00	
W7	29.35 \pm 1.69	\pm 1.07	\pm 1.08	\pm 2.78	\pm 1.84	\pm 5.79	\pm 5.57	\pm 2.24	\pm 0.86	\pm 0.20	\pm 0.03	\pm 0.68	\pm 3.86	\pm 1.00	\pm 0.22	\pm 0.44	\pm 0.01	\pm 2.24
	0.53	0.15	0.21	0.18	0.07	0.44	0.39	1.05	0.12	0.15	0.05	0.22	1.07	0.21	0.12	0.05	0.00	
W8	23.26 \pm 1.20	\pm 0.78	\pm 1.27	\pm 1.65	\pm 1.35	\pm 4.05	\pm 3.55	\pm 1.92	\pm 0.51	\pm 0.95	\pm 0.21	\pm 0.43	\pm 3.69	\pm 1.08	\pm 0.25	\pm 0.37	\pm 0.01	\pm 1.36
	0.04	0.11	0.46	0.10	0.05	0.21	0.03	0.14	0.02	0.11	0.03	0.02	0.42	0.07	0.02	0.04	0.00	
W9	30.65 \pm 1.98	\pm 0.88	\pm 1.45	\pm 4.98	\pm 1.82	\pm 6.08	\pm 3.47	\pm 1.15	\pm 0.77	\pm 0.39	\pm 0.13	\pm 1.64	\pm 4.77	\pm 0.57	\pm 0.30	\pm 0.28	\pm <LOD	\pm 2.71
	0.02	0.06	0.04	1.20	0.35	0.71	0.40	0.16	0.17	0.20	0.10	1.24	2.18	0.25	0.06	0.18		

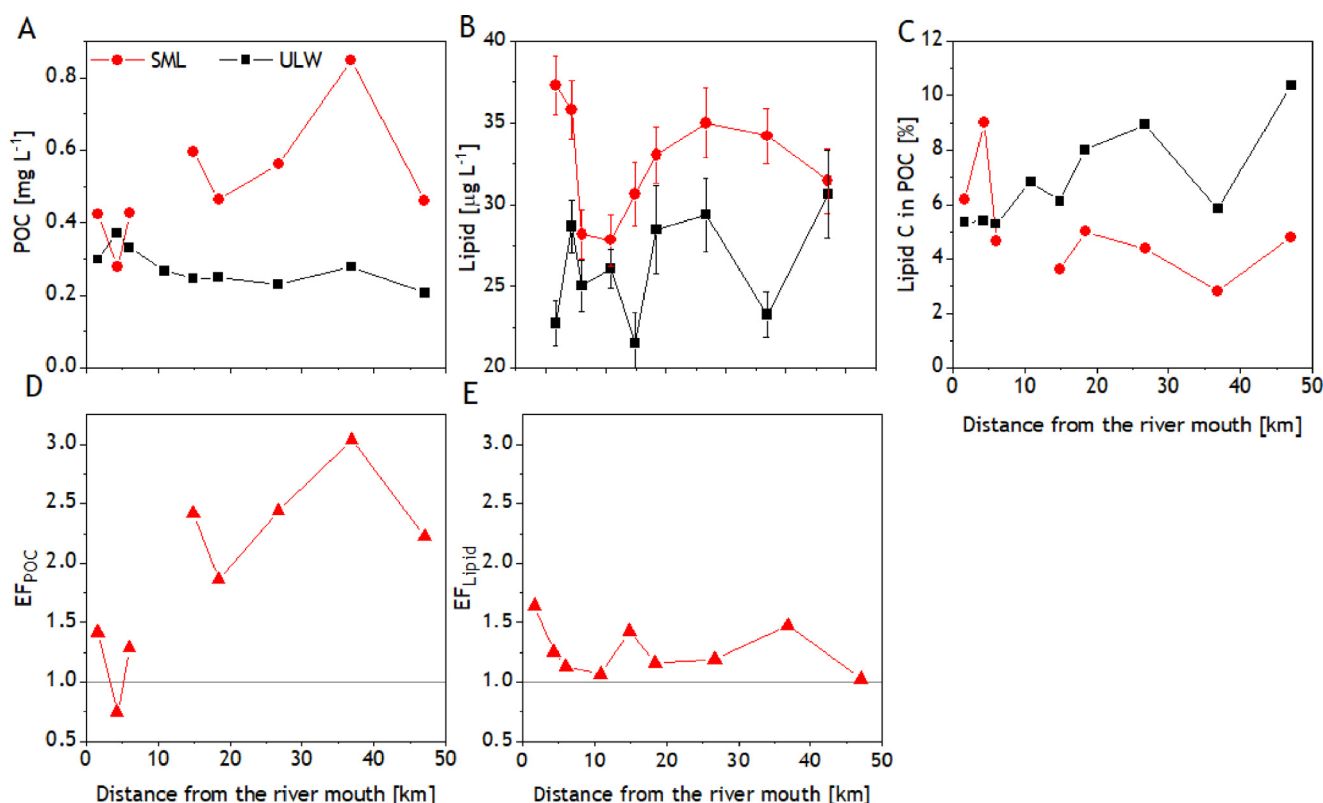


Figure 6 The distribution of particulate organic carbon (POC) (A), particulate lipids (B) and the contribution of particulate lipid carbon to POC (C) in the sea surface microlayer (SML) (circles) and the underlying water (ULW) (squares), along with the enrichment factors (EF) of POC (D) and lipids (E) throughout the transect.

in the SML ranged from 0.27 mg L^{-1} to 0.84 mg L^{-1} , with an average value of $0.51 \pm 0.17 \text{ mg L}^{-1}$, while they were significantly lower in the ULW (two-sample t-test, $p = 0.001$), with an average value of $0.27 \pm 0.05 \text{ mg L}^{-1}$ and ranging from 0.20 mg L^{-1} to 0.37 mg L^{-1} . The lowest POC values in the SML were determined at stations W1–W3, while the highest POC concentrations in the ULW were found at the same stations. POC was enriched in the SML at all stations (1.3–3.0) except station W2 (0.8), with an average enrichment factor of 1.9 ± 0.7 and an increasing trend from the river mouth toward the open sea.

The average concentration of particulate lipids in the SML was $32.60 \pm 3.32 \text{ } \mu\text{g L}^{-1}$, ranging from $27.82 \pm 1.58 \text{ } \mu\text{g L}^{-1}$ to $37.30 \pm 1.79 \text{ } \mu\text{g L}^{-1}$. In the ULW, the average concentration was $26.19 \pm 3.26 \text{ } \mu\text{g L}^{-1}$, much lower than in the SML (two-sample t-test, $p < 0.001$), ranging from $21.50 \pm 1.86 \text{ } \mu\text{g L}^{-1}$ to $30.65 \pm 1.94 \text{ } \mu\text{g L}^{-1}$, with a slightly increasing trend toward the open sea. Particulate lipids were enriched in all SML samples, on average 1.26 ± 0.21 , with the lowest enrichment at station W9 (1.03) and the highest enrichment at station W1 (1.6) (Figure 6). The fraction of particulate lipid carbon in POC ranged from 2.8 to 9.0% (average 5.1%) in the SML and from 5.3 to 10.4% (average 6.9%) in ULW. With the exception of stations W1 and W2, which are closest to the river mouth, the contribution of lipids to POC was higher in the ULW than in the SML, with a statistically significant difference in means, when W1 and W2 are excluded from the analysis (two-sample t-test, $p = 0.003$)

(Figure 6C). The contribution of lipids to POC in the ULW showed an increasing trend toward the open sea.

Lipid classes can be divided into three groups based on their functions. Membrane lipids include the phospholipids (PG, PE and PC) and ST, which are components of planktonic plasma membranes (Cantarero et al., 2020), and the glycolipids (GL): MGDG, DGDG, SQDG, and PIG, which are found in thylakoid membranes and are indicators of autotrophs (Guschina and Harwood, 2009).

Triacylglycerols, WE and ME indicate metabolic reserves of phytoplankton and zooplankton (Arts, 1999). Lipid classes including FFA, ALC, 1,2 DG, 1,3 DG, and MG indicate lipid degradation processes and are referred to as degradation indices (Goutx et al., 2003). The distribution and concentrations of the three groups of lipids are shown in Figure 7. Membrane lipids were the most abundant group, with an average concentration of $19.94 \pm 2.28 \text{ } \mu\text{g L}^{-1}$ in the SML, and $17.78 \pm 2.44 \text{ } \mu\text{g L}^{-1}$ in the ULW. Membrane lipids accounted for an average of $61 \pm 6\%$ of particulate lipids in SML and $68 \pm 4\%$ in ULW, and statistically significant positive correlations were found between the concentrations of PIG ($r = 0.802$, $p = 0.009$), DGDG ($r = 0.677$, $p = 0.045$), SQDG ($r = 0.817$, $p = 0.007$), and PE ($r = 0.768$, $p = 0.015$) in SML and ULW. The average concentration of degradation indices in the SML was $6.79 \pm 1.25 \text{ } \mu\text{g L}^{-1}$, while in the ULW it was $5.35 \pm 0.96 \text{ } \mu\text{g L}^{-1}$, with a statistically significant difference between the two means (two-sample t-test, $p = 0.014$). The degradation indices accounted for an average of $21 \pm 3\%$

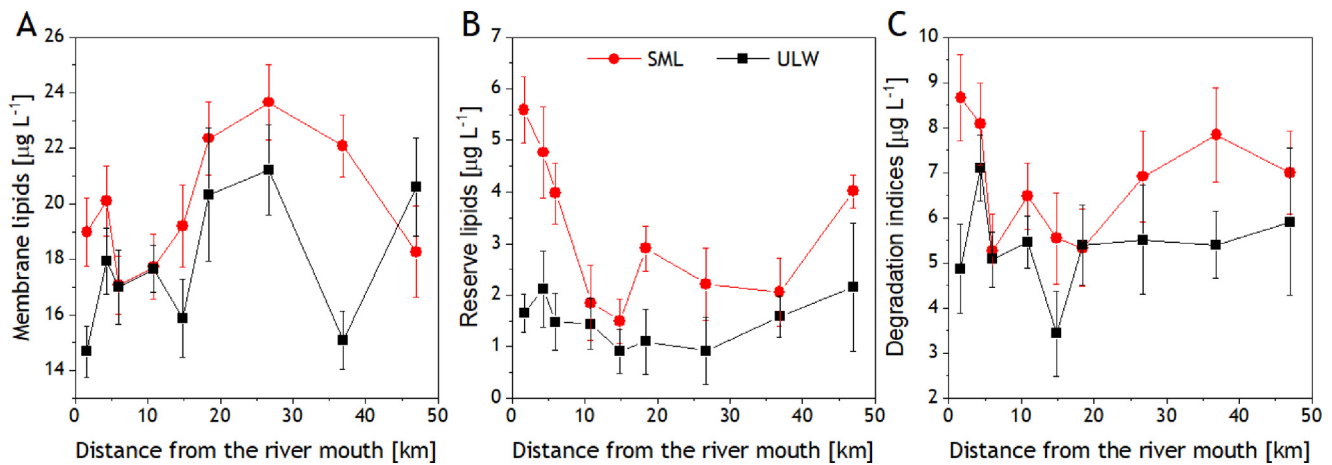


Figure 7 Distribution and concentrations of total membrane lipids (GL, PL, ST and PIG) (A), total reserve lipids (WE, ME and TG) (B) and total degradation indices (FFA, ALC, 1,2 DG, 1,3 DG, MG) (C) in sea surface microlayer (SML) (circles) and underlying water (ULW) (squares) throughout the transect.

and $20 \pm 3\%$ of particulate lipids in SML and ULW, respectively. Statistically significant correlations were found between the concentrations of ALC ($r = 0.762$, $p = 0.017$), 1,3 DG ($r = 0.738$, $p = 0.023$), 1,2 DG ($r = 0.709$, $p = 0.032$), MG ($r = 0.952$, $p < 0.001$) in the SML and ULW.

The lowest concentrations determined were those of reserve lipids, with an average value of $3.21 \pm 1.44 \mu\text{g L}^{-1}$ in the SML and a slightly, but still significantly lower (two-sample t-test, $p = 0.003$) value of $1.48 \pm 0.46 \mu\text{g L}^{-1}$ in the ULW. Reserve lipids accounted for $10 \pm 4\%$ and $6 \pm 2\%$ of the particulate lipids in the SML and ULW, respectively. A statistically significant correlation was found between the concentrations of TG ($r = 0.754$, $p = 0.019$) in SML and ULW.

Hydrocarbons are present in living organisms and account for approximately 1% of the lipid content of marine microorganisms (Sargent et al., 1976). The concentration of hydrocarbons in the particulate fraction ranged from 1.75 to 4.41 $\mu\text{g L}^{-1}$ in the SML and from 1.20 to 1.98 $\mu\text{g L}^{-1}$ in the ULW.

The concentration of glycolipids (MGDS, SQDG and DGDG) increased toward the open sea, especially in the ULW. Oppositely, the concentration of PL in both SML and ULW decreased slightly with distance from the river mouth.

The enrichment in SML was observed for all lipid classes, with reserve lipids showing the highest enrichment, e.g., on average there was 2.9 times more WE in the SML than in the ULW.

Environmental conditions such as nutrient availability, light conditions, and temperature affect the biochemistry of phytoplankton by potentially directing biosynthetic pathways toward the production of different biomolecules, i.e., protein synthesis is favoured under good, non-stressful growth conditions, while lipid synthesis is favoured under stressful conditions (Gašparović et al., 2014, Gerin and Goutx, 1994). The Lipid:Chl a ratio (Gerin and Goutx, 1994) is often used to evaluate the biosynthetic pathways of photosynthetic communities. Using particulate pigment (PIG) concentration data, which provide a rough estimate of autotrophic plankton biomass, we calculated the ratio of particulate lipids and PIG in the SML and ULW (Figure 8). The ratio showed a sharp decrease from stations W1–W2 near

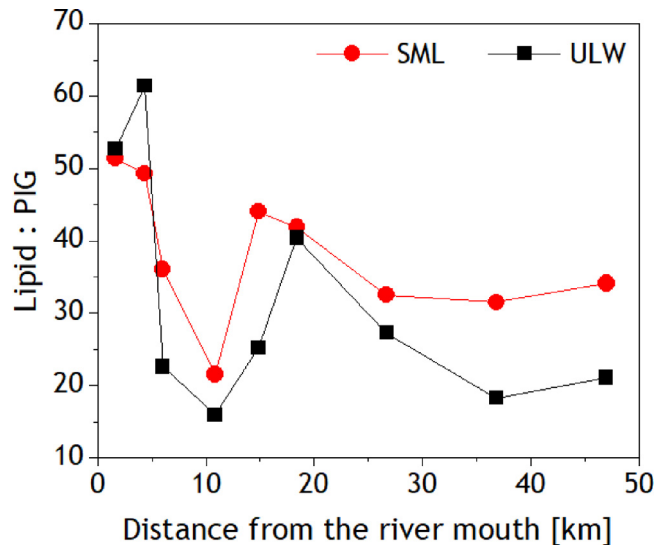


Figure 8 Lipid:PIG ratios in sea surface microlayer (SML) (circles) and underlying water (ULW) (squares) throughout the transect.

the river mouth to stations W3–W4, which are about 5–10 km from the river mouth, after which an increase was observed toward station W5.

The statistically significant negative correlations observed between S_R and the Lipid:PIG ratio in SML ($r = -0.718$, $p = 0.029$) and ULW ($r = -0.795$, $p = 0.010$) (Figure 9) point to a possible relationship between the environmental conditions of phytoplankton growth and the molecular weight of OM produced.

The PE:PG ratios (indicating the predominant bacterial or phytoplankton biomass) (Table S2) ranged from 0.25 to 0.74 in the SML and from 0.33 to 0.91 in the ULW. The highest values were observed at stations W1 and W2 in both SML and ULW, followed by a significant decrease at stations W3 and W4. Wax esters, indicators of zooplankton, were enriched in the SML compared to the ULW (Table 2). The high-

Table 2 Concentration ranges of surface-active organic substances (SAS) and the enrichment factor (EF) ranges in the sea surface microlayer (SML) and underlying water from 1 m depth (ULW), determined in this study, along with results from other similar studies.

Location (sampling method)	SML thickness (μm)	SAS (mg L^{-1} eq. T-X-100)		EF	Reference
		SML	ULW		
Baltic Sea; Vistula plume (metal screen)	~ 500	0.28–0.60	0.22–0.47	1.0–1.4	This study
Middle Adriatic; coastal (metal screen)	260 ± 40	$0.25 \pm 0.06 - 0.79 \pm 0.54$	$0.06 \pm 0.02 - 0.30 \pm 0.13$	1.4–5.1	Frka et al., 2009
W Atlantic; Mauritania (metal screen)	465 ± 34	0.22 ± 0.18	0.16 ± 0.07	1.5 ± 0.7	Barthelmess et al., 2021
North Sea (metal screen)	65–80	0.15–1.96	0.09–1.70	0.9–1.6	Rickard et al., 2022
North Sea (metal screen)	65–80	$0.08 \pm 0.01 - 0.38 \pm 0.04$	$0.09 \pm 0.02 - 0.28 \pm 0.01$	$0.75 \pm 0.17 - 1.90 \pm 0.71$	Pereira et al., 2016.
Norwegian Sea; fjords (metal screen)	100–150	0.12–0.21	0.07–0.14	1.21–2.8	Gašparović et al., 2007.
Baltic Sea and North Sea (glass discs)	60–100	$0.31 \pm 0.03 - 0.60 \pm 0.63$	$0.13 \pm 0.03 - 0.49 \pm 0.05$	$0.9 \pm 0.2 - 3.9 \pm 3.3$	Ribas-Ribas et al., 2017
North Sea; Jade bay (glass discs)	$\sim 50-80$	0.05–0.81	0.20–0.29	0.6–1.0	Rickard et al., 2019
N Atlantic; N Pacific, nearshore (0-2 km) (glass plate)	50–120	0.11–4.99		0.5–5.9	Wurl et al., 2011
N Atlantic; N Pacific, offshore (2-20 km) (glass plate)	50–120	0.11–1.26		0.6–5.0	Wurl et al., 2011
E Pacific; Santa Barbara channel (glass plate)	50 ± 10	0.21–0.83	0.11 – 0.637	3.6–3.9	Wurl et al., 2009
Atlantic transect 2014 (metal screen)		0.12–1.00	0.10–0.36	0.95–4.52	Sabbaghzadeh et al., 2017
Atlantic transect 2015 (metal screen)		0.12–1.76	0.08–0.91	0.97–3.47	Sabbaghzadeh et al., 2017

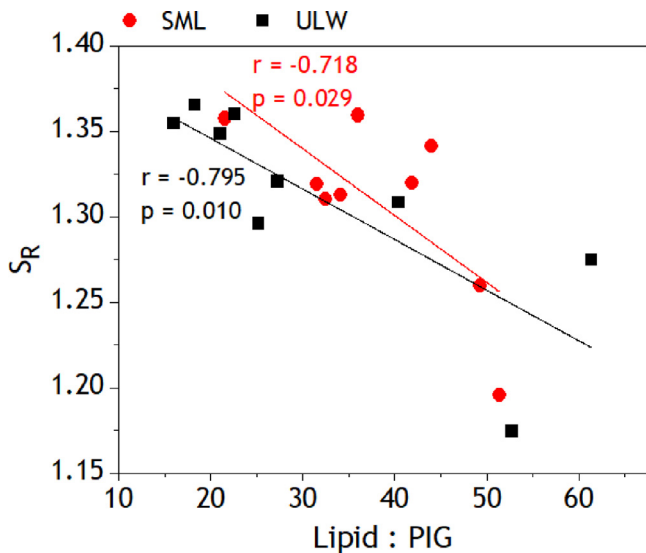


Figure 9 Correlation between the slope ratio (S_R) and the Lipid:PIG ratio for sea surface microlayer (SML) (circles) and underlying water (ULW) (squares) throughout the transect.

est concentration of WE was measured in the SML at station W1, closest to the river mouth.

4. Discussion

4.1. Estimation of river propagation to the Gulf of Gdańsk

In the absence of topographic boundaries, the Vistula Estuary connects freely to the adjacent coastal waters of the Gulf of Gdańsk. The Vistula River plume usually has a horizontal extension of approximately 4–30 km from the river mouth with a thickness between 0.5 and 12 m (Cyberska and Krzywiński, 1988; Grelowski and Wojewodzki, 1996), supplying the Gulf of Gdańsk with terrestrial organic matter. However, the strong northerly winds prior and the easterly winds during the field campaign (Figure S2) caused a strong mixing of the surface waters, probably pushing the Vistula plume westward out of its usual direction (Drozdowska et al., 2017) and increasing salinity to >7 throughout the studied transect. The influence of the river was therefore difficult to discern, and the slight increase in salinity and decrease in temperature from stations W1 and W2 toward the open sea indicated that it was mainly confined to the two stations near the river mouth. As shown by our previous study, which includes this (October 2015) and two other field campaigns (April 2015 and September 2016) along the same transect, the intense mixing of fresh and seawater had an impact on the distribution of OM, based on analysis of its optical properties (Drozdowska et al., 2017). During the April 2015 and September 2016 campaigns, calm, windless sea conditions prevailed, and most importantly, a salinity gradient allowed us to distinguish between coastal waters under the influences of the Vistula River (<7) and seawater (>7), which was not the case during the October 2015 campaign (the

campaign analysed in this study). The most striking differences between April 2015, September 2016 and this campaign were observed for the stations closest to the river mouth. The absorption coefficients $a_{CDOM}(254)$ were higher in April 2015 and September 2016, than in campaign discussed here. The changes in S_R values spanned a range three times larger in April 2015 and September 2016 (Figures 3A, 3B, S3 and S4) (Drozdowska et al., 2017). All FDOM components had significantly higher intensities in both SML and ULW in April 2015 and September 2016 compared to this campaign, especially at stations W1 and W2 (Figures 4 and S5), likely due to calmer weather conditions that allowed for greater influence of riverine material on the surface coastal waters. Fluorescence intensities obtained for this campaign in October 2015, were reasonably comparable to those observed in April 2015 and September 2016 only in waters with salinity >7 , again indicating the very limited influence of the Vistula River and a strong seawater intrusion in October 2015. However, the contribution of the different FDOM components determined in April 2015 and September 2016 was not significantly different from those determined for this campaign, probably because most of the samples in April 2015 and September 2016 actually had salinity >7 .

During the October 2015 campaign, significantly higher $a_{CDOM}(254)$ in the SML and ULW at station W1 compared to all other stations indicate the strongest presence of riverine chromophoric DOM closest to the river mouth, while lower values determined for the two layers at stations W2–W9 indicate the removal of CDOM, probably by photodegradation/transformation (Obenosterer et al., 2008), as well as dilution processes of riverine OM upon entering the Gulf (Pereira et al., 2016). Similar $a_{CDOM}(254)$ absorption coefficient values determined in SML and ULW (Figure 3A) confirmed a well-mixed upper water column, although no statistically significant correlation was found between SML and ULW values.

4.2. Biogeochemistry of SML and ULW

In addition to the optical characterisation from the previous study (Drozdowska et al., 2017), the additional characterization of OM presented in this study helped reveal some biogeochemical processes within the Vistula plume.

The $a_{CDOM}(254)$, an indicator of the presence of aromatic molecules, showed no significant correlation with HC concentrations in SML and ULW, possibly due to the fact that this class of lipids was neither highly aromatic nor of anthropogenic origin, as these mainly have an aromatic structure (Patel et al., 2020). In addition, HC concentrations were below $10 \mu\text{g L}^{-1}$ in both SML and ULW, which is another indication that no significant source of hydrocarbon pollution was present. A slight decrease in $a_{CDOM}(254)$ values with an increasing concentration of SAS observed in the SML, but not in the ULW (Figure S6), suggests that an increase in OM surface activity does not necessarily imply an increase in OM aromaticity, complementing the lack of correlation between $a_{CDOM}(254 \text{ nm})$ and HC.

4.2.1. High wind does not prevent POC accumulation in the SML

Concentrations of POC in our study were comparable to those in other coastal areas (Gašparović et al., 2007,

Penezić et al., 2021, Stolle et al., 2010), but higher than those observed in the Atlantic Ocean (Van Pinxteren et al., 2017). Despite high wind speeds, we observed POC enrichment at all stations except at W2, although no relationship with wind speed was observed. Similar results are obtained by Van Pinxteren et al. (2017), who sampled in both low (2–5) and high ($>5 \text{ m s}^{-1}$) wind conditions. In contrast, Obernosterer et al. (2008) showed a significant negative correlation between POC enrichment in the SML and wind blowing 6 h prior to sampling, where all recorded wind speeds were $<3 \text{ m s}^{-1}$. Stolle et al. (2010), on the other hand, observed the formation of a slick in the southern Baltic Sea at $<2 \text{ m s}^{-1}$ wind speed, which resulted in very high POC concentrations in the SML ($\approx 9 \text{ mg L}^{-1}$), leading to an enrichment factor of up to 26.8.

4.2.2. The active role of surface-active substances in the (re)establishment of SML

The determined concentrations of SAS in the SML and ULW were comparable to those reported by other authors using the same analytical method (calibration with Triton-X-100 as the model compound), for coastal areas, but also for the open sea (Table 2). The same was observed for the enrichment factors, despite different sampling techniques, different locations, weather conditions and different thicknesses of the sampled SML. Despite high wind speeds, SAS were enriched in the SML, although no statistically significant correlation was found between the two parameters. These enrichments confirm the rapid recovery of the SML by transport and accumulation of OM from the subsurface, as observed earlier (Dragičević and Pravdić, 1981; Liss, 1975; Wurl et al., 2009; Sabbaghzadeh et al., 2017). This is particularly evident in the case of SAS that have a high affinity for the air/water interface. A high positive correlation was found between SAS concentrations in the SML and ULW, with a similar linear dependence ($\text{SAS}_{\text{ULW}} = 0.690 \times \text{SAS}_{\text{SML}} + 0.052$) as derived by Pereira et al. (2016) ($\text{SAS}_{\text{ULW}} = 0.766 \times \text{SAS}_{\text{SML}} + 0.018$). Our result supports the observation that ULW constantly replenishes SAS in the SML (Cunliffe et al., 2013; Pereira et al., 2016) and reinforces the discussion about the self-sustainability of the SML with respect to its surface activity, even in strong wind conditions.

4.2.3. Lipids, biomarkers of the trophic conditions

Determined concentrations of particulate lipids in ULW ($21.5\text{--}30.6 \mu\text{g L}^{-1}$) and SML ($27.8\text{--}37.3 \mu\text{g L}^{-1}$) are generally lower compared to other studies of mostly more oligotrophic areas (e.g., Penezić et al., 2010 ($47.9 \mu\text{g L}^{-1}$ particulate lipids in SML and $46.4 \mu\text{g L}^{-1}$ in ULW); Triesch et al., 2021 (concentrations of particulate lipids: $36.4\text{--}93.5 \mu\text{g L}^{-1}$ in SML and $61.0\text{--}118.1 \mu\text{g L}^{-1}$ in ULW)). However, lipid enrichments were observed at all stations (Figure 6E).

Significantly higher concentrations of total lipids, reserve lipids, and degradation indices in SML compared to ULW (Figures 6 and 7, Table 1) indicated a richer plankton community in the SML than in the ULW, although non-living OM may have contributed to both POC and lipid pools. This suggests the Baltic SML as the layer of more favourable trophic conditions for plankton development. The SML enrichment

of reserve lipids (Figure 7B) suggests that the plankton in the SML grew under more stressful conditions compared to the ULW, because these lipids are known to accumulate in phytoplankton under adverse environmental conditions, whereas optimal phytoplankton growth usually results in lower lipid cell content (Bourguet et al., 2009; Novak et al., 2019; Sharma et al., 2012). In particular, conditions such as lack of nutrients, as well as an increase in temperature can influence lipid composition and production, which usually leads to an accumulation of lipids (Novak et al., 2018; Sharma et al., 2012). The observed increase in GL concentration with increasing distance from the river mouth, especially evident in the ULW, can be related to the expected decrease in nutrient concentration at greater distance from the Vistula Estuary (Pastuszak et al., 2012) and points to one of the adaptive mechanisms of phytoplankton to low nutrient conditions, namely intensified synthesis of phosphorus- and nitrogen-free molecules such as glycolipids MGDG, SQDG, and DGDG (Frka et al., 2011). On the other hand, the decreasing concentrations of PL with increasing distance from the river mouth indicate a lower availability of phosphorus, since the synthesis of phospholipids depends on P availability.

The trophic conditions of a system can also be indicated by the contribution of particulate lipids to POC, which can exceed 30% in oligotrophic conditions (Frka et al., 2011; Marić et al., 2013; Gašparović et al., 2014). The low contribution of lipids to POC found in this study (Figure 6c), as low as 2.8% and predominantly less than 10%, is more characteristic for eutrophic areas. The change in trophic conditions along the transect was observed by an increasing contribution of lipids in the POC with increasing distance from the river mouth observed in the ULW. In the ULW the contribution of lipid to POC was generally higher than in the SML, especially at stations W3 to W9. The lower contribution of lipids to POC observed in SML suggests that nutrients were more available to phytoplankton in the SML than in the ULW, except at stations close to the river mouth (W1 and W2). This is plausible considering that OM degradation and remineralization are faster in SML due to biotic (bacteria) (Tank et al., 2011; Zhang et al., 2013b) and especially abiotic (photooxidation and autoxidation by free radical-mediated oxidation (Rontani and Belt, 2020)) processes. Higher concentrations of lipid degradation indices in SML (Figure 7c) confirm higher OM degradation and remineralization in this layer, while the presence, but not the enrichment, of bacterial biomarker PE in SML confirms the importance of the simultaneous effects of abiotic OM processing in the SML (Table 2). In addition, according to Reinthaler et al. (2008), bacterial growth in the SML is low and bacterioneuston only maintains its cellular mass, while Stolle et al. (2010) found that the productivity of the bacterioneuston is not, or only weakly, associated with the change in the amount of OM in SML.

4.2.4. OM origin

Statistically significant correlations between the concentrations of PIG, DGDG, SQDG, and PE in SML and ULW, suggest that the ULW was the origin of plankton lipid classes in the SML, rather than the presence of independent plankton populations in the two layers. The enrichment of membrane

lipids (Figure 7A) confirms the enrichment of living plankton in the SML (Derieux et al., 1998).

While PE are the most abundant phospholipids in marine bacteria (Gerin and Goutx, 1993), PG are the major phospholipids in microalgae (Dembitsky and Rozentsvet, 1990; Harwood, 2006). The PE:PG ratio is thus used as an indicator of bacterial or phytoplankton biomass dominance; PE:PG ratios between 0 and 0.3 indicate phytoplankton dominance, and >0.3 bacterial dominance (Gerin and Goutx, 1994). The values of PE:PG ratio, which were mostly above 0.3 in the transect (Table S2), indicate a significant presence of bacteria in both layers (Table S2), while a statistically significant positive correlation between the concentrations of PE in the SML and ULW points to the interconnection of the two layers. The highest ratios observed for W1 and W2 in both SML and ULW indicate the highest bacterial biomass, probably supported by riverine originated OM and nutrients.

The high PIG concentrations detected in both SML and ULW samples at 10 km from the river mouth (station W4, Table 2), indicated rich phytoplankton biomass, most likely due to good growing conditions. The evaluated low Lipid:PIG ratios (Figure 8) suggested reduced lipid accumulation expected for plankton growth under optimal environmental conditions (e.g. Novak et al., 2019). An increase in the contribution of the “T” component in the fluorescence intensities at station W4 from an average of 14% to 18% (Figure 4C and D) in SML and from an average of 15% to 18% in ULW, indicated the presence of freshly produced proteinaceous material, further confirming significant plankton activity at W4. This observation was possible because the measurements were performed in unfiltered samples, which allowed detection of the freshly produced proteinaceous material that tends to form gel-like structures and would otherwise have been retained on the filter (Drozdowska et al., 2018). The highest values of the (M+T):(A+C) ratio (Table S2) observed at station W4 also indicated a slightly higher contribution of OM of marine origin at this station, compared to the other stations, likely due to the assumed increase in primary production.

In addition to indicating the photochemically induced shift in molecular weight (Helms et al., 2008), S_R can also be used as an indicator of phytoplankton biomass, leading to an increase in autochthonous OM that contains a higher proportion of low molecular weight compounds (Santos-Echeandía et al., 2012; Zhang et al., 2013b). A significant increase in S_R at stations W3 and W4 (Figure 3B) also suggested an increase in phytoplankton primary production. The statistically significant negative correlation between S_R and the Lipid:PIG ratio (Figure 9) underlined that primary production was directed toward the production of lower molecular weight OM by phytoplankton growing under favourable environmental conditions.

The lowest observed (M+T):(A+C) ratio that was determined at station W1 in the ULW provided a slight indication of a higher contribution of terrestrial humic substances of high molecular weight. However, based on the (M+T):(A+C) ratios, which averaged 0.57 in the SML and 0.56 in the ULW, OM can only be classified as being of mixed marine and terrestrial/anthropogenic origin (Drozdowska et al., 2015; Osburn et al., 2014). Another indication of the dominance of higher molecular weight terrestrial OM at stations W1 and

W2 was the lowest observed S_R slope ratio determined for the ULW and SML.

Wax esters, primarily reserve lipids of zooplankton with amphiphilic properties, may dominate the reserve lipid pool in freshwater zooplankton (Arts, 1999). The WE detected in our samples most likely originated from the microzooplankton, since the samples were prefiltered with a net with a pore size of 200 μm . The active movement of microzooplankton toward a richer food source in SML resulted in WE having one of the highest enrichments in the SML compared to all other lipid classes analysed.

5. Conclusions

Characterization of OM along the transect in the eutrophic coastal area of the Gulf of Gdańsk, partially encompassing the Vistula River plume, provided insights into the biogeochemical processes affecting the OM distribution in the SML and ULW.

The rapid establishment of SML in strong winds was confirmed by the enrichment of SAS and POC detected even at the highest wind speeds and throughout the transect, while the highly positive, statistically significant correlation between SAS concentrations in the SML and ULW indicated the rapid resupply of SAS in the SML from the ULW.

Due to the wind blowing before and during the campaign, the small influence exerted by the Vistula River within the studied transect was limited to a few kilometres narrow area near the river mouth (stations W1 and somewhat W2), as shown mainly by the optical properties of OM. Station W1 was characterized by the highest values of the absorption coefficient at 254 nm in both SML and ULW, together with the lowest S_R ratios observed at W1 and W2, indicating the highest contribution of aromatic and high molecular weight molecules as well as terrestrial visible humic-like substances, implied by the highest observed fluorescence intensities at W1 and W2. The highest concentrations of total particulate lipids in SML, especially groups comprising reserve lipids and degradation indices, were detected at W1 and W2, pointing to intense degradation processes in the surface microlayer, which was further confirmed by the highest observed PE:PG ratios in the SML and ULW, as an indicator of high bacterial biomass. The enrichment of lipid degradation indices in the SML and the lack of the bacterial biomarker PE enrichment, suggest that OM was subjected to more abiotic (photooxidation and autoxidation) and/or biotic reworking/remineralization processes in the SML than in the ULW. The most intense biological activity was observed at W4, as indicated by the highest PIG concentrations and the lowest Lipid:PIG ratio in the SML and ULW. Analysis of the distribution of the Lipid:PIG ratio led to the observation of a statistically significant negative correlation between the S_R and the Lipid:PIG ratio in both SML and ULW, linking the favourable environmental conditions for phytoplankton growth to the production of lower molecular weight OM.

The complexity of physical, chemical, and biochemical factors, including photochemistry, winds, biological productivity and activity, that determine OM distribution, makes it difficult to show a clear (de)coupling between SML and ULW. However, our observations with respect to specific classes

and groups of OM suggest that the ULW is the major supplier of OM to the SML, leading to its enrichment by some OM classes. The similar distribution in SML and ULW and the lack of “enrichment” of optical indices point to the similar type of material in both layers, which potentially lacks significant surface activity. Thus, the coupling of SML and ULW is highly dependent on the specific properties of the analysed OM as well as external factors. The relationships and dependencies shown here represent a valuable step toward better understanding the biogeochemistry of surface coastal waters.

Declaration of competing interest

The authors declare that they have no known competing financial interests or personal relationships that could have appeared to influence the work reported in this paper.

Acknowledgements

We thank the crew of the r/v *Oceania*. This work was funded by a grant from the Croatian Science Foundation under projects IP-11-2013-8607 and IP-2018-01-3105, and by the Polish National Science Centre contract No. 2021/41/B/ST10/00946. We would also like to thank the reviewers, whose comments and insights deeply helped to improve the quality of the manuscript.

Supplementary materials

Supplementary material associated with this article can be found, in the online version, at <https://doi.org/10.1016/j.oceano.2022.05.003>.

References

- Andrén, E., 1999. Changes in the composition of the diatom flora during the last century indicate increased eutrophication of the Oder estuary, south-western Baltic Sea. *Estuar. Coast. Shelf Sci.* 48 (6), 665–676. <https://doi.org/10.1006/ecss.1999.0480>
- Archer, C.L., Jacobson, M.Z., 2005. Evaluation of global wind power. *J. Geophys. Res. Atmos.* 110, D1110. <https://doi.org/10.1029/2004JD005462>
- Arrigo, K.R., Brown, C.W., 1996. Impact of chromophoric dissolved organic matter on UV inhibition of primary productivity in the sea. *Mar. Ecol. Prog. Ser.* 140, 207–216. <https://doi.org/10.3354/meps140207>
- Arts, M.T., 1999. Lipids in Freshwater Zooplankton: Selected Ecological and Physiological Aspects. In: Arts, M.T., Wainman, B.C. (Eds.), *Lipids in Freshwater Ecosystems*. Springer, New York, NY, 71–90. https://doi.org/10.1007/978-1-4612-0547-0_5
- Barthelmess, E.T., Schütte, F., Engel, A., 2021. Variability of the Sea Surface microlayer Across a filament’s edge and potential influences on gas exchange. *Front. Mar. Sci.* 8, 718384. <https://doi.org/10.3389/fmars.2021.718384>
- Belanger, S., Babin, M., Larouche, P., 2008. An empirical ocean color algorithm for estimating the contribution of chromophoric dissolved organic matter to total light absorption in optically complex waters. *J. Geophys. Res.* 113, C04027. <https://doi.org/10.1029/2007JC004436>
- Bligh, E.G., Dyer, W.J., 1959. A rapid method of total lipid extraction and purification. *Can. J. Biochem. Physiol.* 37, 911–917. <https://doi.org/10.1139/y59-099>
- Bourguet, N., Goutx, M., Ghiglione, J.F., Pujo-Pay, M., Mevel, G., Momzikoff, A., Mousseau, L., Guigue, C., Garcia, N., Raimbault, P., Pete, R., Oriol, L., Lefevre, D., 2009. Lipid biomarkers and bacterial lipase activities as indicators of organic matter and bacterial dynamics in contrasted regimes at the DYFAMED site, NW Mediterranean. *Deep-Sea Res. Pt. II* 56, 1454–1469. <https://doi.org/10.1016/j.dsr2.2008.11.034>
- Broecker, H.-C., Petermann, J., Siems, W., 1978. The influence of wind on CO₂-exchange in a wind-wave tunnel, including the effects of monolayers. *J. Mar. Res.* 36, 595–610.
- Bruggemann, M., Hayeck, N., George, C., 2018. Interfacial photochemistry at the ocean surface is a global source of organic vapors and aerosols. *Nat. Commun.* 9, 2101. <https://doi.org/10.1038/s41467-018-04528-7>
- Buszewski, B., Buszewska, T., Chmarzyński, A., Kowalkowski, T., Kowalska, J., Kosobucki, P., Zbytniewski, R., Namieśnik, J., Kot-Wasik, A., Pacyna, J., Panasiuk, D., 2005. The present condition of the Vistula River catchment area and its impact on the Baltic Sea coastal zone. *Reg. Environ. Chang.* 5, 97–110. <https://doi.org/10.1007/s10113-004-0077-8>
- Cantarero, S.I., Henríquez-Castillo, C., Dildar, N., Vargas, C.A., von Dassow, P., Cornejo-D’Ottone, M., Sepúlveda, J., 2020. Size-Fractionated Contribution of Microbial Biomass to Suspended Organic Matter in the Eastern Tropical South Pacific Oxygen Minimum Zone. *Front. Mar. Sci.* 7, 1–20. <https://doi.org/10.3389/fmars.2020.540643>
- Coble, P.G., 1996. Characterization of marine and terrestrial DOM in seawater using excitation-emission matrix spectroscopy. *Mar. Chem.* 51, 325–346. [https://doi.org/10.1016/0304-4203\(95\)00062-3](https://doi.org/10.1016/0304-4203(95)00062-3)
- Coble, P.G., 2007. *Marine optical biogeochemistry: The chemistry of ocean color*. *Chem. Rev.* 107, 402–418. [10.1021/cr050350+](https://doi.org/10.1021/cr050350+)
- Ćosović, B., Vojvodić, V., Pleše, T., 1985. Electrochemical determination and characterization of surface active substances in freshwaters. *Water Res.* 19, 175–183. [https://doi.org/10.1016/0043-1354\(85\)90196-4](https://doi.org/10.1016/0043-1354(85)90196-4)
- Ćosović, B., Vojvodić, V., 1998. Voltammetric analysis of surface active substances in natural seawater. *Electroanalysis* 10, 429–434. [https://doi.org/10.1002/\(SICI\)1521-4109\(199805\)10:6<429::AID-ELAN429>3.0.CO;2-7](https://doi.org/10.1002/(SICI)1521-4109(199805)10:6<429::AID-ELAN429>3.0.CO;2-7)
- Ćosović, B., 2005. Surface-Active Properties of the Sea Surface Microlayer and Consequences for Pollution in the Mediterranean Sea. *The Handbook of Environmental Chemistry*. Springer <https://doi.org/10.1007/b107150>
- Cunliffe, M., Engel, A., Frka, S., Gašparović, B., Guitart, C., Murrell, J.C., Salter, M., Stolle, C., Upstill-Goddard, R., Wurl, O., 2013. Sea surface microlayers: A unified physicochemical and biological perspective of the air-ocean interface. *Prog. Oceanogr.* 109, 104–116. <https://doi.org/10.1016/j.pocan.2012.08.004>
- Cyberska, B., Krzymiński, W., 1988. Extension of the Vistula River water in the Gulf of Gdańsk. In: *Proc. 16th Conf. Baltic Oceanograph. Instit. Mar. Res., Kiel, Germany*, 290–304.
- Dembitsky, V.M., Rozentsvet, O.A., 1990. Phospholipid composition of some marine red algae. *Phytochemistry* 29, 3149–3152. [https://doi.org/10.1016/0031-9422\(90\)80175-G](https://doi.org/10.1016/0031-9422(90)80175-G)
- Derieux, S., Fillaux, J., Saliot, A., 1998. Lipid class and fatty acid distributions in particulate and dissolved fractions in the north Adriatic Sea. *Org. Geochem.* 29, 5–7. [https://doi.org/10.1016/S0146-6380\(98\)00089-8](https://doi.org/10.1016/S0146-6380(98)00089-8)
- Dragičević, D., Pravdić, V., 1981. Properties of the seawater–air interface: Rates of surface film formation under steady state conditions. *Limnol. Oceanogr.* 26, 492–499. <https://doi.org/10.4319/lo.1981.26.3.0492>
- Drozdowska, V., Babichenko, S., Lisin, A., 2002. Natural water fluorescence characteristics based on lidar investigations of a sur-

- face water layer polluted by an oil film; the Baltic cruise – May 2000. *Oceanologia* 44 (3), 339–354.
- Drozdowska, V., 2007. Seasonal and spatial variability of surface seawater fluorescence properties in the Baltic and Nordic Seas: Results of lidar experiments. *Oceanologia* 49 (1), 59–69.
- Drozdowska, V., Fateyeva, N.L., 2013. Spectrophotometric study of natural Baltic surfactants – results of marine experiment. In: Traczewska, T.M., Hanus-Lorenz, B. (Eds.), *Hydrobiology in Environment Protection*. Oficyna Wydawnicza Politechniki Wrocławskiej, Wrocław, 25–32.
- Drozdowska, V., Józefowicz, M., 2015. Spectrophotometric studies of marine surfactants in the southern Baltic Sea. *Oceanologia* 57 (2), 159–167. <https://doi.org/10.1016/j.oceano.2014.12.002>
- Drozdowska, V., Kowalczyk, P., Józefowicz, M., 2015. Spectrofluorometric characteristics of fluorescent dissolved organic matter in a surface microlayer in the Southern Baltic coastal waters. *J. Eur. Opt. Soc.* 10, 15050. <https://doi.org/10.2971/jeos.2015.15050>
- Drozdowska, V., Wrobel, I., Markuszewski, P., Makuch, P., Raczkowska, A., Kowalczyk, P., 2017. Study on organic matter fractions in the surface microlayer in the Baltic Sea by spectrophotometric and spectrofluorometric methods. *Ocean Sci.* 13, 633–647. <https://doi.org/10.5194/os-13-633-2017>
- Drozdowska, V., Kowalczyk, P., Konik, M., Dzierzbicka-Głowacka, L., 2018. Study on different fractions of organic molecules in the Baltic Sea surface microlayer by spectrophotometric and spectrofluorimetric methods. *Front. Mar. Sci.* 5, 1–12. <https://doi.org/10.3389/fmars.2018.00456>
- Engel, A., Bange, H.W., Cunliffe, M., Burrows, S.M., Friedrichs, G., Galgani, L., Herrmann, H., Hertkorn, N., Johnson, M., Liss, P.S., Quinn, P.K., Schartau, M., Soloviev, A., Stolle, C., Upstill-Goddard, R.C., van Pinxteren, M., Zäncker, B., 2017. The Ocean's vital skin: toward an integrated understanding of the sea surface microlayer. *Front. Mar. Sci.* 4. <https://doi.org/10.3389/fmars.2017.00165>
- Falkowska, L., 1999. Sea surface microlayer: A field evaluation of teflon plate, glass plate and screen sampling techniques. Part 2. Dissolved and suspended matter. *Oceanologia* 41 (2), 223–240.
- Frew, N.M., Goldman, J.C., Dennett, M.R., Johnson, A.S., 1990. Impact of phytoplankton-generated surfactants on air-sea gas exchange. *J. Geophys. Res.* 95, 3337. <https://doi.org/10.1029/jc095ic03p03337>
- Frka, S., Kozarac, Z., Čosović, B., 2009. Characterization and seasonal variations of surface active substances in the natural sea surface micro-layers of the coastal Middle Adriatic stations. *Estuar. Coast. Shelf Sci.* 85, 555–564. <https://doi.org/10.1016/j.ecss.2009.09.023>
- Frka, S., Gašparović, B., Marić, D., Godrijan, J., Djakovac, T., Vojvodić, V., Dautović, J., Kozarac, Z., 2011. Phytoplankton driven distribution of dissolved and particulate lipids in a semi-enclosed temperate sea (Mediterranean): Spring to summer situation. *Estuar. Coast. Shelf Sci.* 93 (4), 290–304. <https://doi.org/10.1016/j.ecss.2011.04.017>
- Gašparović, B., Kozarac, Z., Saliot, A., Čosović, B., Möbius, D., 1998. Physico-chemical characterization of natural and ex-situ reconstructed sea-surface microlayers. *J. Colloid Interface Sci.* 208, 191–202. <https://doi.org/10.1006/jcis.1998.5792>
- Gašparović, B., Plavšić, M., Čosović, B., Saliot, A., 2007. Organic matter characterization in the sea surface microlayers in the subarctic Norwegian fjords region. *Mar. Chem.* 105, 1–14. <https://doi.org/10.1016/j.marchem.2006.12.010>
- Gašparović, B., Djakovac, T., Tepić, N., Degobbis, D., 2011. Relationships between surface-active organic substances, chlorophyll a and nutrients in the northern Adriatic Sea. *Cont. Shelf Res.* 31, 1149–1160. <https://doi.org/10.1016/j.csr.2011.04.010>
- Gašparović, B., Frka, S., Koch, B.P., Zhu, Z.Y., Bracher, A., Lechtenfeld, O.J., Neogi, S.B., Lara, R.J., Kattner, G., 2014. Factors influencing particulate lipid production in the East Atlantic Ocean. *Deep-Sea Res. Pt. I.* 89, 56–67. <https://doi.org/10.1016/j.dsr.2014.04.005>
- Gašparović, B., Kazazić, S.P., Cvitešić, A., Penezić, A., Frka, S., 2015. Improved separation and analysis of glycolipids by latroscan thin-layer chromatography-flame ionization detection. *J. Chromatogr. A* 1409, 259–267. <https://doi.org/10.1016/j.chroma.2015.07.047>
- Gašparović, B., Penezić, A., Lampitt, R.S., Sudasinghe, N., Schaub, T., 2016. Free fatty acids, tri-, di- and monoacylglycerol production and depth-related cycling in the Northeast Atlantic. *Mar. Chem.* 186, 101–109. <https://doi.org/10.1016/j.marchem.2016.09.002>
- Gašparović, B., Kazazić, S.P., Cvitešić, A., Penezić, A., Frka, S., 2017. Corrigendum to “Improved separation and analysis of glycolipids by latroscan thin-layer chromatography–flame ionization detection”. [*J. Chromatogr. A* 1409 (2015) 259267. <https://doi.org/10.1016/j.chroma.2015.07.047>]. *J. Chromatogr. A* 1521. <https://doi.org/10.1016/j.chroma.2017.09.038>
- Gašparović, B., Penezić, A., Frka, S., Kazazić, S., Lampitt, R.S., Holguin, F.O., Sudasinghe, N., Schaub, T., 2018. Particulate sulfur-containing lipids: production and cycling from the epipelagic to the abyssopelagic zones. *Deep-Sea Res. Pt. I* 134, 12–22. <https://doi.org/10.1016/j.dsr.2018.03.007>
- Gerin, C., Goutx, M., 1993. Separation and quantification of phospholipids from marine bacteria with the latroscan mark IV TLC–FID. *J. Planar Chromatogr.* 6, 307–312.
- Gerin, C., Goutx, M., 1994. Latroscan-measured particulate and dissolved lipids in the Almeria-Oran frontal system (Almofront-1, May 1991). *J. Mar. Sys.* 5, 343–360. [https://doi.org/10.1016/0924-7963\(94\)90055-8](https://doi.org/10.1016/0924-7963(94)90055-8)
- Giani, M., Savelli, F., Berto, D., Zangrando, V., Čosović, V., Vojvodić, V., 2005. Temporal dynamics of dissolved and particulate organic carbon in the northern Adriatic Sea in relation to the mucilage events. *Sci. Total Environ.* 353, 126–138. <https://doi.org/10.1016/j.scitotenv.2005.09.062>
- Glasby, G.P., Szefer, P., 1998. Marine pollution in Gdansk Bay, Puck Bay and the Vistula Lagoon, Poland: An overview. *Sci. Total Environ.* 212, 49–57. [https://doi.org/10.1016/S0048-9697\(97\)00333-1](https://doi.org/10.1016/S0048-9697(97)00333-1)
- Goutx, M., Guigue, C., Striby, L., 2003. Triacylglycerol biodegradation experiment in marine environmental conditions: Definition of a new lipolysis index. *Org. Geochem.* 34, 1465–1473. [https://doi.org/10.1016/S0146-6380\(03\)00119-0](https://doi.org/10.1016/S0146-6380(03)00119-0)
- Grelowski, A., Wojewodzki, T., 1996. The impact of the Vistula river on the hydrological conditions in the Gulf of Gdansk in 1994. *Bull. Sea Fish. Inst.* 137, 23–33.
- Guschina, I.A., Harwood, J.L., 2009. Algal lipids and effect of the environment on their biochemistry. In: Kainz, M., Brett, M.T., Arts, M.T. (Eds.), *Lipids in Aquatic Ecosystems*. Springer, New York, 1–24. https://doi.org/10.1007/978-0-387-89366-2_1
- Harvey, H.R., Tuttle, J.H., Bell, J., 1995. Kinetics of phytoplankton decay during simulated sedimentation, Changes in biochemical composition and microbial activity under oxic and anoxic conditions. *Geochim. Cosmochim. Acta* 59, 367–3377. [https://doi.org/10.1016/0016-7037\(95\)00217-N](https://doi.org/10.1016/0016-7037(95)00217-N)
- Harwood, J.L., 2006. Membrane Lipids in Algae. In: Siegenthaler, P.-A., Murata, N. (Eds.), *Lipids in Photosynthesis: Structure, Function and Genetics*. Advances in Photosynthesis and Respiration, vol 6. Springer, Dordrecht, 53–64. https://doi.org/10.1007/0-306-48087-5_3
- HELCOM, 2018. Input of nutrients by the seven biggest rivers in the Baltic Sea region. *Balt. Sea Environ. Proc. No.* 161, 31. <https://www.helcom.fi/wp-content/uploads/2019/08/BSEP163.pdf>
- Helms, J.R., Stubbins, A., Ritchie, J.D., Minor, E.C., Kieber, D.J., Mopper, K., 2008. Absorption spectral slopes and slope ratios as indicators of molecular weight, source, and photobleaching of chromophoric dissolved organic matter. *Limnol. Oceanogr.* 53, 955–969. <https://doi.org/10.4319/lo.2008.53.3.0955>

- Hunter, K.A., 1997. Chemistry of the sea-surface microlayer. In: Liss, P.S., Duce, R.A. (Eds.), *The sea surface and global change*. Cambridge Univ. Press., 287–320.
- Johannessen, S.C., Miller, W.L., 2001. Quantum yield for the photochemical production of dissolved inorganic carbon in seawater. *Mar. Chem.* 76, 271–283. [https://doi.org/10.1016/S0304-4203\(01\)00067-6](https://doi.org/10.1016/S0304-4203(01)00067-6)
- Kowalczyk, P., Stedmon, C.A., Markager, S., 2006. Modeling absorption by CDOM in the Baltic Sea from season, salinity and chlorophyll. *Mar. Chem.* 101, 1–11. <https://doi.org/10.1016/j.marchem.2005.12.005>
- Kruk-Dowgiallo, L., 1996. The role of the filamentous brown algae in the degradation of the underwater meadows the Gulf of Gdańsk. *Oceanol. Stud.* 25, 125–135.
- Larsson, U., Elmgren, R., Wulff, F., 1985. Eutrophication and the Baltic sea: Causes and consequences. *Ambio* 14, 9–14.
- Lei, X., Pan, J., Devlin, A.T., 2020. Variations of the Absorption of Chromophoric Dissolved Organic Matter in the Pearl River Estuary. In *Estuaries and Coastal Zones-Dynamics and Response to Environmental Changes*. IntechOpen. <https://www.intechopen.com/chapters/70692>
- Liss, P.S., 1975. Chemistry of the sea surface microlayer. In: Riley, J.P., Skirrow, G. (Eds.), *Chemical Oceanography*, vol. 2. Academic Press, London, U.K., 193–244.
- Liss, P.S., Duce, R.A. (Eds.), 1997, *The Sea Surface and Global Change*. Cambridge Univ. Press, New York, 519 pp. <https://doi.org/10.1017/CBO9780511525025>
- Loiselle, S.A., Bracchini, L., Dattilo, A.M., Ricci, M., Tognazzi, A., Cózar, A., Rossi, C., 2009. Optical characterization of chromophoric dissolved organic matter using wavelength distribution of absorption spectral slopes. *Limnol. Oceanogr.* 54, 590–597. <https://doi.org/10.4319/lo.2009.54.2.0590>
- Maksymowska, D., Richard, P., Piekarek-Jankowska, H., Riera, P., 2000. Chemical and isotopic composition of the organic matter sources in the Gulf of Gdansk (Southern Baltic Sea). *Estuar. Coast. Shelf Sci.* 51, 585–598. <https://doi.org/10.1006/ecss.2000.0701>
- Marcinek, S., Santinelli, C., Cindrić, A.M., Evangelista, V., Gonnelli, M., Layglon, N., Mounier, S., Lenoble, V., Omanović, D., 2020. Dissolved organic matter dynamics in the pristine Krka River estuary (Croatia). *Mar. Chem.* 225, 103848. <https://doi.org/10.1016/j.marchem.2020.103848>
- Marić, D., Frka, S., Godrijan, J., Tomažić, I., Penezić, A., Djakovac, T., Vojvodić, V., Precali, R., Gašparović, B., 2013. Organic matter production during late summer-winter period in a temperate sea. *Cont. Shelf Res.* 55, 52–65. <https://doi.org/10.1016/j.csr.2013.01.008>
- Mayer, K.J., Wang, X., Santander, M.V., Mitts, B.A., Sauer, J.S., Sultana, C.M., Cappa, C.D., Prather, K.A., 2020. Secondary marine aerosol plays a dominant role over primary sea spray aerosol in cloud formation. *ACS Cent. Sci.* 6, 2259–2266. <https://doi.org/10.1021/acscentsci.0c00793>
- Mazur-Marzec, H., Krężel, A., Kobos, J., Pliński, M., 2006. Toxic *Nodularia spumigena* blooms in the coastal waters of the Gulf of Gdańsk: a ten-year survey. *Oceanologia* 48 (2), 255–273.
- Murphy, K.R., Butler, K.D., Spencer, R.G.M., Stedmon, C.A., Boehme, J.R., Aiken, G.R., 2010. Measurement of dissolved organic matter fluorescence in aquatic environments: An inter-laboratory comparison. *Environ. Sci. Technol.* 44, 9405–9412. <https://doi.org/10.1021/es102362t>
- Mustaffa, N.I.H., Ribas-Ribas, M., Banko-Kubis, H.M., Wurl, O., 2020. Global reduction of in situ CO₂ transfer velocity by natural surfactants in the sea-surface microlayer. *Proc. R. Soc. A* 476, 20190763. <https://doi.org/10.1098/rspa.2019.0763>
- Novak, T., Godrijan, J., Pfannkuchen, D.M., Djakovac, T., Mlakar, M., Baricevic, A., Tanković, M.S., Gašparović, B., 2018. Enhanced dissolved lipid production as a response to the sea surface warming. *J. Mar. Sys.* 180, 289–298. <https://doi.org/10.1016/j.jmarsys.2018.01.006>
- Novak, T., Godrijan, J., Pfannkuchen, D.M., Djakovac, T., Medić, N., Ivančić, I., Mlakar, M., Gašparović, B., 2019. Global warming and oligotrophication lead to increased lipid production in marine phytoplankton. *Sci. Total Environ.* 668, 171–183. <https://doi.org/10.1016/j.scitotenv.2019.02.372>
- Obernosterer, I., Catala, P., Lami, R., Caparros, J., Ras, J., Bricaud, A., Dupuy, C., Van Wambeke, F., Lebaron, P., 2008. Biochemical characteristics and bacterial community structure of the sea surface microlayer in the South Pacific Ocean. *Biogeosciences* 5, 693–705. <https://doi.org/10.5194/bg-5-693-2008>
- Osburn, C.L., Del Vecchio, R., Boyd, T.J., 2014. Physicochemical effects on dissolved organic matter fluorescence in natural waters. In: Coble, P.G., Lead, J., Baker, A., Reynolds, D.M., Spencer, R.G.M. (Eds.), *Aquatic Organic Matter Fluorescence*. Cambridge Univ. Press, New York, 233–277.
- Parlanti, E., Wörz, K., Geoffroy, L., Lamotte, M., 2000. Dissolved organic matter fluorescence spectroscopy as a tool to estimate biological activity in a coastal zone submitted to anthropogenic inputs. *Org. Geochem.* 31, 1765–1781. [https://doi.org/10.1016/S0146-6380\(00\)00124-8](https://doi.org/10.1016/S0146-6380(00)00124-8)
- Parrish, C.C., 1988. Dissolved and particulate marine lipid classes: a review. *Mar. Chem.* 23 (1–2), 17–40. [https://doi.org/10.1016/0304-4203\(88\)90020-5](https://doi.org/10.1016/0304-4203(88)90020-5)
- Parrish, C.C., Abrajano, T.A., Budge, S.M., Helleur, R.J., Hudson, E.D., Pulchan, K., Ramos, C., 2000. Lipid and Phenolic Biomarkers in Marine Ecosystems: Analysis and Applications. In: Wangersky, P.J. (Ed.), *Marine Chemistry. The Handbook of Environmental Chemistry*, vol 5D. Springer, Berlin, Heidelberg https://doi.org/10.1007/10683826_8
- Pastuszak, M., Stålnacke, P., Pawlikowski, K., Witek, Z., 2012. Response of Polish rivers (Vistula, Oder) to reduced pressure from point sources and agriculture during the transition period (1988–2008). *J. Mar. Sys.* 94, 157–173. <https://doi.org/10.1016/j.jmarsys.2011.11.017>
- Patel, A.B., Shaikh, S., Jain, K.R., Desai, C., Madamwar, D., 2020. Polycyclic Aromatic Hydrocarbons: Sources, Toxicity, and Remediation Approaches. *Front. Microbiol.* 11, 562813. <https://doi.org/10.3389/fmicb.2020.562813>
- Peđziński, J., Witak, M., 2019. Evidence of cultural eutrophication of the Gulf of Gdańsk based on diatom analysis. *Oceanol. Hydrobiol. Stud.* 48, 247–261. <https://doi.org/10.2478/ohs-2019-0022>
- Penezić, A., Gašparović, B., Burić, Z., Frka, S., 2010. Distribution of marine lipid classes in salty Rogoznica Lake (Croatia). *Estuar. Coast. Shelf Sci.* 86, 625–636. <https://doi.org/10.1016/j.ecss.2009.11.030>
- Penezić, A., Milinković, A., Bakija Alempijević, S., Žužul, S., Frka, S., 2021. Atmospheric deposition of biologically relevant trace metals in the eastern Adriatic coastal area. *Chemosphere* 283, 131178. <https://doi.org/10.1016/j.chemosphere.2021.131178>
- Pereira, R., Schneider-Zapp, K., Upstill-Goddard, R.C., 2016. Surfactant control of gas transfer velocity along an offshore coastal transect: results from a laboratory gas exchange tank. *Biogeosciences* 13, 3981–3989. <https://doi.org/10.5194/bg-13-3981-2016>
- Piskozub, J., Drozdowska, V., Irczuk, M., 1998. A water Raman extinction lidar system for detecting thin oil spills: preliminary results of field tests. *Oceanologia* 40 (1), 3–10.
- Reinthal, T., Sintes, E., Herndl, G.J., 2008. Dissolved organic matter and bacterial production and respiration in the sea-surface microlayer of the open Atlantic and the western mediterranean sea. *Oceanogr.* 53 (1), 122–136. <https://doi.org/10.4319/lo.2008.53.1.0122>
- Ribas-Ribas, M., Mustaffa, N.I.H., Rahlff, J., Stolle, C., Wurl, O., 2017. Sea surface scanner (S3): A catamaran for high-resolution

- measurements of biogeochemical properties of the sea surface microlayer. *J. Atmos. Ocean. Technol.* 34, 1433–1448. <https://doi.org/10.1175/JTECH-D-17-0017.1>
- Rickard, P.C., Uher, G., Upstill-Goddard, R.C., Frka, S., Mustaffa, N.I.H., Banko-Kubis, H.M., Cvitešić Kušan, A., Gašparović, B., Stolle, C., Wurl, O., Ribas-Ribas, M., 2019. Reconsideration of seawater surfactant activity analysis based on an inter-laboratory comparison study. *Mar. Chem.* 208, 103–111. <https://doi.org/10.1016/j.marchem.2018.11.012>
- Rickard, P.C., Uher, G., Upstill-Goddard, R.C., 2022. Photo-reactivity of surfactants in the sea-surface microlayer and subsurface water of the Tyne estuary, UK. *Geophys. Res. Lett.* 49 (4), e2021GL095469. <https://doi.org/10.1029/2021GL095469>
- Robinson, T.B., Wurl, O., Bahlmann, E., Jürgens, K., Stolle, C., 2019. Rising bubbles enhance the gelatinous nature of the air–sea interface. *Limnol. Oceanogr.* 64, 2358–2372. <https://doi.org/10.1002/lno.11188>
- Romankevich, E.A., 1984. *Geochemistry of Organic Matter in the Ocean*. Springer Berlin, Heidelberg, 334.
- Rontani, J.F., Belt, S.T., 2020. Photo- and autoxidation of unsaturated algal lipids in the marine environment: An overview of processes, their potential tracers, and limitations. *Org. Geochem.* 139, 103941. <https://doi.org/10.1016/j.orggeochem.2019.103941>
- Ryba, A.S., Burgess, R.M., 2002. Effects of sample preparation on the measurement of organic carbon, hydrogen, nitrogen, sulfur and oxygen concentrations in marine sediments. *Chemosphere* 48, 139–147. [https://doi.org/10.1016/s0045-6535\(02\)00027-9](https://doi.org/10.1016/s0045-6535(02)00027-9)
- Sabbaghzadeh, B., Upstill-Goddard, R.C., Beale, R., Pereira, R., Nightingale, P.D., 2017. The Atlantic Ocean surface microlayer from 50°N to 50°S is ubiquitously enriched in surfactants at wind speeds up to 13 m s⁻¹. *Geophys. Res. Lett.* 44, 2852–2858. <https://doi.org/10.1002/2017GL072988>
- Salter, M.E., Upstill-Goddard, R.C., Nightingale, P.D., Archer, S.D., Blomquist, B., Ho, D.T., Huebert, B., Schlosser, P., Yang, M., 2011. Impact of an artificial surfactant release on air-sea gas fluxes during Deep Ocean Gas Exchange Experiment II. *J. Geophys. Res. Oceans* 116, C11016. <https://doi.org/10.1029/2011JC007023>
- Santos-Echeandía, J., Caetano, M., Brito, P., Canario, J., Vale, C., 2012. The relevance of defining trace metal baselines in coastal waters at a regional scale: The case of the Portuguese coast (SW Europe). *Mar. Environ. Res.* 79, 86–99. <https://doi.org/10.1016/j.marenvres.2012.05.010>
- Sargent, J.R., Lee, R.F., Nevenzel, J.C., 1976. Marine waxes. In: Kolattukudy, P.E. (Ed.), *Chemistry and Biochemistry of Natural Waxes*. Elsevier, Amsterdam, 49–91.
- Schiewer, U., Schernewski, G., 2002. Baltic Coastal Ecosystem Dynamics and Integrated Coastal Zone Management. In: Ass, E.-P. (Ed.), *Littoral 2002, Proc. 6th International Symposium, Porto 22–26.9.2002*. Univ. Porto, 115–123.
- Schneider-Zapp, K., Salter, M.E., Mann, P.J., Upstill-Goddard, R.C., 2013. Technical Note: Comparison of storage strategies of sea surface microlayer samples. *Biogeosciences* 10, 4927–4936. <https://doi.org/10.5194/bg-10-4927-2013>
- Sharma, K.K., Schuhmann, H., Schenk, P.M., 2012. High lipid induction in microalgae for biodiesel production. *Energies* 5, 1532–1553. <https://doi.org/10.3390/en5051532>
- Stedmon, C.A., Markager, S., Kaas, H., 2000. Optical properties and signatures of chromophoric dissolved organic matter (CDOM) in Danish coastal waters. *Estuar. Coast. Shelf Sci.* 51, 267–278. <https://doi.org/10.1006/ecss.2000.0645>
- Stedmon, C.A., Markager, S., Bro, R., 2003. Tracing dissolved organic matter in aquatic environments using a new approach to fluorescence spectroscopy. *Mar. Chem.* 82, 239–254. [https://doi.org/10.1016/S0304-4203\(03\)00072-0](https://doi.org/10.1016/S0304-4203(03)00072-0)
- Stefan, R.L., Szeri, A.J., 1999. Surfactant scavenging and surface deposition by rising bubbles. *J. Colloid Interface Sci.* 212, 1–13. <https://doi.org/10.1006/jcis.1998.6037>
- Stolle, C., Nagel, K., Labrenz, M., Jürgens, K., 2010. Succession of the sea-surface microlayer in the coastal Baltic Sea under natural and experimentally induced low-wind conditions. *Biogeosciences* 7, 2975–2988. <https://doi.org/10.5194/bg-7-2975-2010>
- Stolle, C., Ribas-Ribas, M., Badewien, T.H., Barnes, J., Carpenter, L.J., et al., 2020. The Milan Campaign: Studying diel light effects on the air-sea interface. *Bull. Am. Meteorol. Soc.* 101, 146–166. <https://doi.org/10.1175/BAMS-D-17-0329.1>
- Szymczak-Żyła, M., Krajewska, M., Witak, M., Ciesielski, T.M., Ardelan, M.V., Jenssen, B.M., Goslar, T., Winogradow, A., Filipkowska, A., Lubecki, L., Zamojska, A., Kowalewska, G., 2019. Present and Past-Millennial Eutrophication in the Gulf of Gdańsk (Southern Baltic Sea). *Paleoceanogr. Paleoclimatology* 34, 136–152. <https://doi.org/10.1029/2018PA003474>
- Tank, S.E., Lesack, L.F.W., Gareis, J.A.L., Osburn, C.L., Hesslein, R.H., 2011. Multiple tracers demonstrate distinct sources of dissolved organic matter in lakes of the Mackenzie delta, western Canadian Arctic. *Limnol. Oceanogr.* 56 (4), 1297–1309. <https://doi.org/10.4319/lo.2011.56.4.1297>
- Triesch, N., van Pinxteren, M., Frka, S., Spranger, T., Hoffmann, E.H., Gong, X., Wex, H., Schulz-Bull, D., Gašparović, B., Herrmann, H., 2021. Concerted measurements of lipids in seawater and on submicron aerosol particles at the Cape Verde Islands: biogenic sources, selective transfer and high enrichments. *Atmos. Chem. Phys.* 21, 4267–4283. <https://doi.org/10.5194/acp-21-4267-2021>
- Tsai, W.-T., Lui, K.-K., 2003. An assessment of the effects of seasurface surfactant on global atmosphere-ocean CO₂ flux. *J. Geophys. Res.* 108, 3127–3143. <https://doi.org/10.1029/2000JC000740>
- Van Pinxteren, M., Barthel, S., Fomba, K.W., Müller, K., Von Tümpling, W., Herrmann, H., Thomsen, L., 2017. The influence of environmental drivers on the enrichment of organic carbon in the sea surface microlayer and in submicron aerosol particles—measurements from the Atlantic Ocean. *Elementa: Science of the Anthropocene* 5, 35. <https://doi.org/10.1525/elementa.225>
- Williams, P.M., Carlucci, A.F., Henrichs, S.M., Van Fleet, E.S., Horri-gan, S.G., Reid, F.M.H., Robertson, K.J., 1986. Chemical and microbiological studies of sea-surface films in the Southern Gulf of California and off the West Coast of Baja California. *Mar. Chem.* 19, 17–98. [https://doi.org/10.1016/0304-4203\(86\)90033-2](https://doi.org/10.1016/0304-4203(86)90033-2)
- Woolf, D.K., 2005. Bubbles and their role gas exchange. In: Liss, P.S., Duce, R.A. (Eds.), *The Sea Surface and Global Change*. Cambridge Univ. Press, U. K, 173–205.
- Wurl, O., Obbard, J.P., 2004. A review of pollutants in the sea-surface microlayer (SML): A unique habitat for marine organisms. *Mar. Pollut. Bull.* 48, 1016–1030. <https://doi.org/10.1016/j.marpolbul.2004.03.016>
- Wurl, O., Miller, L., Röttgers, R., Vagle, S., 2009. The distribution and fate of surface-active substances in the sea-surface microlayer and water column. *Mar. Chem.* 115, 1–9. <https://doi.org/10.1016/j.marchem.2009.04.007>
- Wurl, O., Wurl, E., Miller, L., Johnson, K., Vagle, S., 2011. Formation and global distribution of sea-surface microlayers. *Biogeosciences* 8, 121–135. <https://doi.org/10.5194/bg-8-121-2011>
- Wurl, O., Ekau, W., Landing, W.M., Zappa, C.J., 2017. Sea surface microlayer in a changing ocean – A perspective. *Elem. Sci. Anthropocene* 5, 31. <https://doi.org/10.1525/elementa.228>
- Zhang, Z., Liu, L., Liu, C., Cai, W., 2003. Studies on the sea surface microlayer: II. The layer of sudden change of physical and chemical properties. *J. Colloid Interf. Sci.* 264, 148–159. [https://doi.org/10.1016/S0021-9797\(03\)00390-4](https://doi.org/10.1016/S0021-9797(03)00390-4)
- Zhang, Y., Liu, X., Osburn, C.L., Wang, M., Qin, B., Zhou, Y., 2013a. Photobleaching Response of Different Sources of Chromophoric

- Dissolved Organic Matter Exposed to Natural Solar Radiation Using Absorption and Excitation-Emission Matrix Spectra. *PLoS One* 8, e77515. <https://doi.org/10.1371/journal.pone.0077515>
- Zhang, Y., Liu, X., Wang, M., Qin, B., 2013b. Compositional differences of chromophoric dissolved organic matter derived from phytoplankton and macrophytes. *Org. Geochem.* 55, 26–37. <https://doi.org/10.1016/j.orggeochem.2012.11.007>
- Zhao, J., Cao, W., Xu, Z., Ai, B., Yang, Y., Jin, G., Wang, G., Zhou, W., Chen, Y., Chen, H., Sun, Z., 2018. Estimating CDOM concentration in highly turbid estuarine coastal waters. *J. Geophys. Res.-Oceans* 123, 5856–5873. <https://doi.org/10.1029/2018JC013756>